JUACEP Summer Program 2018 at Nagoya University

Japan-US-Canada Advanced Collaborative Education Program

Nagoya University

Table of Contents

<1> About the Program

(a) Overview

Summer 10-week course 2018 for the students of University of Michigan, UCLA and University of Toronto

Duration: June 19 – August 30, 2018
Research presentations: The 22nd JUACEP Workshop on August 27, 2018

This program is designed for graduate students of University of Michigan, University of California, Los Angeles and University of Toronto.

Each participant chose a research laboratory at Nagoya University in accordance with his/her research interest and carried out a research project under the supervisor of the laboratory. At the same time most of them attended the Japanese language class, the hands-on engine model assembly course and some special events organized for the program.

During the program period, they took part in the labs' events such as seminars, sessions, trips, casual parties, and so on. Teaching Assistants (TA) assigned by the program supported the participants not only in research scenes but also in daily life.

At the end of the program, they submitted the research report to the supervisors and gave the final presentation at the 22nd JUACEP Workshop, which took place at NIC Conference Hall on August 27. Based on evaluations of the report and the presentation by each supervisor, the participants were recognized 2-3 credits by Nagoya University, which are transferred as graduation credits for the students of University of Michigan.

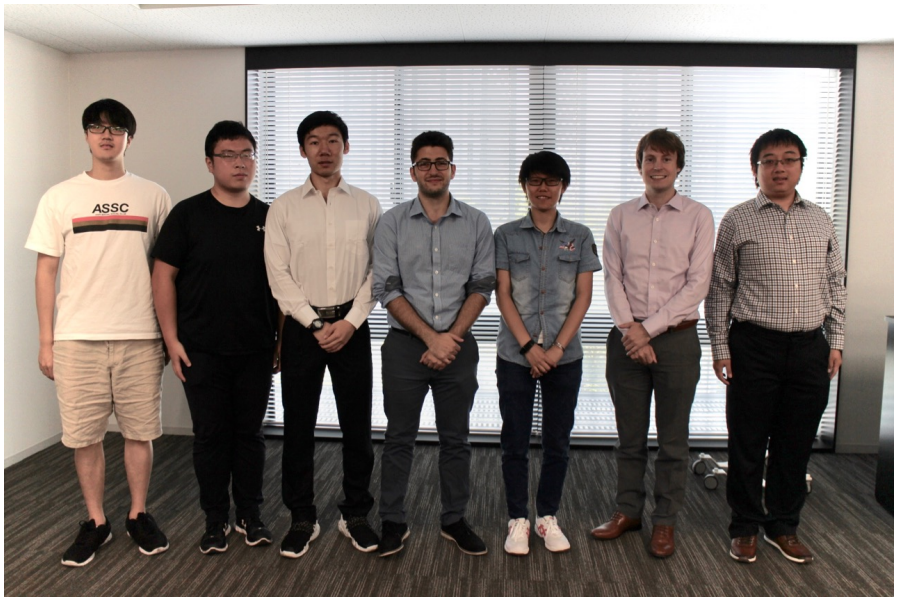

All participants at the 22nd Workshop on August 27, 2018

(b) Participants

	Name	Adviser & Teaching Assistant at NU
1	**Ziming Song** Civil and Environmental Engineering, Univ. Michigan	Assoc. Prof. Tomio Miwa TA: Jiang Feng Civil Engineering
2	**Sida Li** Electrical and Computer Engineering, UCLA	Assoc. Prof.Kiichi Niitsu TA: Atsuki Kobayashi Electrical Engineering
3	**Fadi Rafeedi** Mechanical and Aerospace Engineering, UCLA	Prof. Yasuhisa Hasegawa TA: Mengze Li Micro-Nano Mechanical Science and Engineering
4	**Xuan Yang** Mechanical and Aerospace Engineering, UCLA	Prof. Yoji YAMADA TA: Yohsuke Kuboki Mechanical Systems Engineering
5	**Guanqun Yang** Electrical and Electronics Engineering, UCLA	Prof. Yoji YAMADA TA: Eugene Kim Mechanical Systems Engineering
6	**Chenhui Zhou** Materials and Science Engineering, UCLA	Prof. Noritaka Usami TA: Soichiro Kamibeppu Materials Process Engineering
7	**Petrus Verberne** Mechanical Industrial Engineering, Univ. Toronto	Prof. Yang Ju TA:Takuto Taguchi Micro-Nano Mechanical Science and Engineering

Japanese Course Instructors

Ms. Sumie Yasui
TA: Sinpeng Songlod and Yuri Saito

Coordinators of Partner Universities

Prof. Katsuo Kurabayashi
Mechanical Engineering, University of Michigan

Prof. Jenn-Ming Yang
Materials Science and Engineering, UCLA

Prof. Shaker Meguid
Mechanical Industrial Engineering, University of Toronto

JUACEP Members

Prof. Yang Ju
Micro-Nano Mechanical Science and Engineering

Prof. Noritsugu Umehara
Micro-Nano Mechanical Science and Engineering

Prof. Toshiro Matsumoto
Mechanical Systems Engineering

Assoc. Prof. Yasumasa Ito
Mechanical Systems Engineering

Assoc. Prof. Takayuki Tokoroyama
Micro-Nano Mechanical Science and Engineering

Tomoko Kato
Administrative staff

(c) JUACEP Summer Program 2018 Schedule

Day	Date		8:45-10:15	10:30-12:00		13:00-14:30	14:45-16:15	16:30-
1	June 18	Mon	Arrival at International Residence Yamate					
2	June 19	Tue	10:20 Reception - Orientation @ES Hall		Lunch	13:00 Stipend @Acct office	Lab introduction @ each Lab	
3	June 20	Wed	Research @ each Lab			Research @ each Lab		
4	June 21	Thu				13:45-16:15 Jp Class① @EB-N, IB101		
5	June 22	Fri				Research @ each Lab		
6	June 23	Sat						
7	June 24	Sun						
8	June 25	Mon	Research @ each Lab			Research @ each Lab		
9	June 26	Tue				13:45-16:15 Jp Class② @EB-N, IB101		
10	June 27	Wed				Research @ each Lab		
11	June 28	Thu				13:45-16:15 Jp Class③ @EB-N, IB101		
12	June 29	Fri				Research @ each Lab		
13	June 30	Sat						
14	July 1	Sun						
15	July 2	Mon	Research @ each Lab			Research @ each Lab		
16	July 3	Tue				13:45-16:15 Jp Class④ @EB-N, IB101		
17	July 4	Wed				13:00 Stipend @Acct office	Research @ each Lab	
18	July 5	Thu				13:45-16:15 Jp Class⑤ @EB-N, IB101		
19	July 6	Fri				Research @ each Lab		
20	July 7	Sat						
21	July 8	Sun						
22	July 9	Mon	Research @ each Lab			13:00 Hands-on, B @ EB-N, Creation Plaza, 10F		
23	July 10	Tue				13:45-16:15 Jp Class⑥ @EB-N, IB101		
24	July 11	Wed				Research @ each Lab		
25	July 12	Thu				13:00 45th Seminar(E)		
26	July 13	Fri				Research @ each Lab		16:30 Meet-up @EB-2N424
27	July 14	Sat						
28	July 15	Sun						
29	July 16	Mon	(Marine day)					
30	July 17	Tue	Research @ each Lab			13:45-16:15 Jp Class⑦ @EB-N, IB101		
31	July 18	Wed				Research @ each Lab		
32	July 19	Thu				13:45-16:15 Jp Class⑧ @EB-N, IB101		
33	July 20	Fri				Research @ each Lab		
34	July 21	Sat						
35	July 22	Sun						
36	July 23	Mon	Research @ each Lab			Research @ each Lab		
37	July 24	Tue				13:45-16:15 Jp Class⑨ @EB-N, IB101		
38	July 25	Wed				Research @ each Lab		
39	July 26	Thu				13:45-16:15 Jp Class Final @EB-N, IB101		
40	July 27	Fri	Field Trip, Meeting at Toyota Auditorium at 9:00am					
41	July 28	Sat						
42	July 29	Sun						
43	July 30	Mon	Research @ each Lab			Research @ each Lab		
44	July 31	Tue						
45	Aug 1	Wed						
46	Aug 2	Thu						
47	Aug 3	Fri				13:00 Stipend @Acct office		
48	Aug 4	Sat						
49	Aug 5	Sun						
50	Aug 6	Mon	Research @ each Lab			Research @ each Lab		
51	Aug 7	Tue						
52	Aug 8	Wed						
53	Aug 9	Thu						
54	Aug 10	Fri						
55	Aug 11	Sat						
56	Aug 12	Sun						
57	Aug 13	Mon	(Bon Holidays)					
58	Aug 14	Tue						
59	Aug 15	Wed	Research @ each Lab			Research @ each Lab		
60	Aug 16	Thu						
61	Aug 17	Fri						
62	Aug 18	Sat						
63	Aug 19	Sun						
64	Aug 20	Mon	Research @ each Lab			Research @ each Lab		
65	Aug 21	Tue	Research @ each Lab	Discussion with JM. Yang				
66	Aug 22	Wed	Research @ each Lab					
67	Aug 23	Thu	Research @ each Lab					
68	Aug 24	Fri						
69	Aug 25	Sat						
70	Aug 26	Sun						
71	Aug 27	Mon	22nd Workshop @ NIC Meeting Room, 3F			Research @ each Lab		
72	Aug 28	Tue	Research @ each Lab					
73	Aug 29	Wed						
74	Aug 30	Thu	Closing Session					
75	Aug 31	Fri	Departure from Residence Yamate					

JUACEP event	Japanese class		Stipend payment	Holiday

<2> Research Achievements

(a) Research Internship ---Research Reports

Name	Report title, *Adviser at Nagoya Univ.*	Page
Ziming Song	"Optimization of Rural Bus Network in Toyota City" *Assoc. Prof. Tomio Miwa, Civil Engineering*	9
Sida Li	"Gate Leakage Based Timer Design for Biomedical Devices" *Assoc. Prof.Kiichi Niitsu, Electrical Engineering* *(Undisclosed)*	14
Fadi Rafeedi	"Controlling Flower Stick Rotation Using 3D Vision Feedback" *Prof. Yasuhisa Hasegawa, Micro-Nano Mechanical Science and Engineering (Undisclosed)*	15
Xuan Yang	"A Study on Autonomous Motion Planning of Mobile Robot by Use of Deep Reinforcement Learning for Fall Prevention in Hospital" *Prof. Yoji Yamada, Mechanical Systems Engineering*	16
Guanqun Yang	"The Change of Gait Motion During Curvilinear Obstacle Avoidance while Restricted by a Wearable Robotic Device" *Prof. Yoji Yamada, Mechanical Systems Engineering*	23
Chenhui Zhou	"Aluminum Induced Crystallization of Silicon Thin Film on Strontium Titanate Substarate" *Prof. Noritaka Usami, Materials Process Engineering*	27
Petrus Verberne	"Investigating the Mechanical Properties of CNT Sheet Films" *Prof. Yang Ju, Micro-Nano Mechanical Science and Engineering*	32

OPTIMIZATION OF RURAL BUS NETWORK IN TOYOTA CITY

Ziming Song

Department of Industrial and Operation Engineering,
Division of Integrative Systems and Design,
College of Engineering, University of Michigan
songzm@umich.edu

Supervisor: Tomio Miwa

Graduate School of Engineering, Nagoya University
miwa@nagoya-u.ac.jp

ABSTRACT

In this report, we investigated the rural bus network of the Toyota city. The current bus network in rural region of Toyota city is inefficient, unnecessary transfer is often required. The optimization focus to reduce the waste in the bus network of Toyota city. In this paper we briefly introduced the different optimization algorithms and how different algorithm can be apply to the bus route optimization problem. In this paper the problem formulation is discussed, and objective selection is investigated. The preliminary results show the optimized bus network has 22.2% cost saving in terms of the operating cost.

1. INTRODUCTION

Toyota City is a major city situated in Aichi Prefecture of Japan. According to the data by prefectural government of Aichi the Toyota City is the biggest city of the Aichi Prefecture in terms of the square area. However according to the data from Aichi government, the population is only above 400000 people [1]. Therefore, there are some rural area in the Toyota city which are sparsely populated. According to a survey data, the majority of the population in sparsely populated areas are the elderly people. Elderly population have some of the basic transportation needs such as grocery shopping at the supermarket and doctor visits. In this study, we will focus the bus network in the Asahi region of the Toyota city [2]. The elderly population lives in the Asahi region, however if they want to visit the doctor or shopping in the super market, they have to visit Asuke another region of the Toyota city. Following Figure illustrate the current bus network

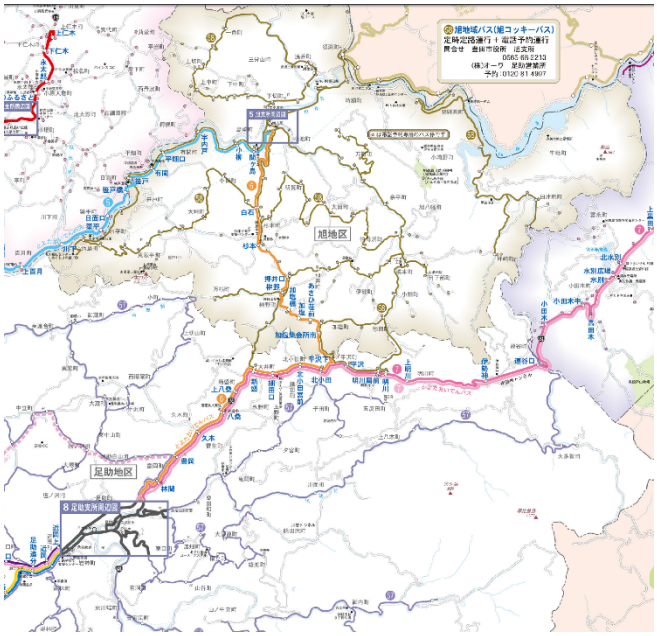

Figure 1 Current Bus Network in Asahi Region of Toyota City [2]

As the above figure, the current bus network in Asahi region involve the Key Bus (Kikan) lines and Branch lines. In the current bus network setup, if an elderly need to travel to Asuke to see the doctors, first they need to take the branch lines to the center of Asahi then take the key bus to the Asuke. Under current network setup, the elderly will have to travel for a long time on the branch lines to the center of Asahi then take the key lines to the Asuke. Therefore, this setup is cost ineffective and time consuming. To resolve above problem, the optimization of the bus network in Asahi region is needed. In this study we will be investigating several optimization algorithms, we will discuss the formulation of the problem, we will be identifying the best objective for optimization

from the objective selection process, we will be also discuss some of the possible solution to the bus network optimization problem. The optimization of the network will eliminate the transfer between key routes and branch routes. As the optimized service will connect directly between rural area of Asahi and center of the Asuke.

2. OPTIMIZATION ALGORITHMS

In an optimization problem, there are multiple algorithms can solve or provide approximate solutions. In this bus network optimization problem there are several algorithms can be applied. One of the algorithms is classical linear program. Linear program is a mathematical program focus on get the optimum solution under a series of the constraints. The standard form of linear program is described in below sets of equations:

$$Maximize\ C^T x \tag{1}$$

$$subject\ to\ Ax \leq b \tag{2}$$

$$0 \leq x \tag{3}$$

Another optimization model that apply to the bus network optimization problem is the transportation model. The transportation model is a special linear program model that deal with the shipping passengers or goods from sources to the destinations. The objective for the original transportation model is to minimize while satisfying the supply and demand in the transport network. Following figure illustrates a basic transportation network

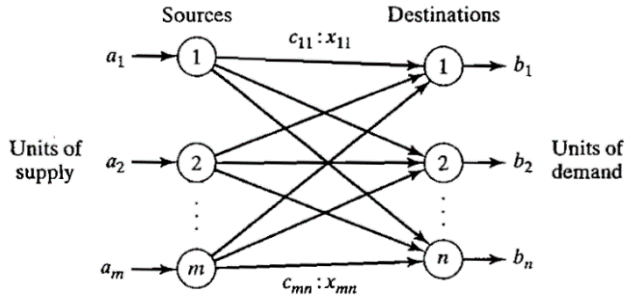

Figure 2 Sample Transportation network [3]

In addition to classical linear optimization models, there are some other nonlinear models that can be applied to this problem. Such models include Traveling Salesman Model and heuristics models. Traveling salesman problem deals with find shortest total travel distance in a n city tour. One of the constraints of traveling salesman problem is to only have each city visited once therefore this algorithm could be useful to the problem we are investigating. The typical formulation of traveling salesman problem is shown below[4]:

$$x_{ij} = \begin{cases} 1, if\ city\ j\ is\ reached\ from\ city\ i \\ 0, otherwise \end{cases} \tag{4}$$

$$Minimize\ z = \sum_{i=1}^{n}\sum_{j=1}^{n} d_{ij}x_{ij}, d_{ij} = \infty\ for\ all\ i\ and\ j \tag{5}$$

subject to

$$\sum_{j=1}^{n} x_{ij} = 1,\ i = 1,2,\dots,n \tag{6}$$

$$\sum_{i=1}^{n} x_{ij} = 1,\ i = 1,2,\dots,n \tag{7}$$

$$x_{ij} = (0,1) \tag{8}$$

A modified traveling salesman problem can be applied to the optimization problem we are investigating. The classical traveling salesman problem only allows every city to be visited once but, in our problem, the terminal stations needs to be visited for every trip. Therefore, a modified traveling salesman problem can apply to our problem.

Heuristics algorithm is a algorithm that does not seek the optimum solution but looking for a good solution. The heuristics algorithm includes the methods such as simulated annealing and genetic algorithm. In a complex optimization such as route optimization problem, sometimes it is impossible to get the absolute optimum solution. However, the heuristics can help to get a good solution without being the most optimum one. Compare to the other algorithm, the heuristics algorithm usually takes longer to compute [3].

From the above optimization algorithms, we can conclude that the modified traveling salesman problem is the best algorithm to use in our case. Although the computation requires some computation power.

3. PROBLEM FORMULATION

From the algorithm section above, the modified traveling salesman algorithm is the key to solve this bus route optimization problem. For the traveling salesman problem, the formulation in the previous section shows the standard formulation. However according to the problem statement, the constraints needs to be modified to fit the problem. One of the constraints that needs to be modified is the city constraint. In the classical traveling salesman problem, each city can be only visited for once. However, in our case two stops which includes the shopping center and hospital in the Asuke needs to be visited for every round trip due to the fact the bus users usually traveling to these two stops. In addition to the stop constraints, the capacity constraints need to be added into the problem formulation. In the Asuke and Asahi region of the Toyota city, most of the roads are in the mountainous region therefore the bus size is severely limited do the road condition. For the safety reason the maximum capacity for each bus is limited to the 19 passengers. As the

safety requirement, the maximum capacity constraint needs to be added into the formulation of this optimization problem.

4. OBJECTIVE SELECTION

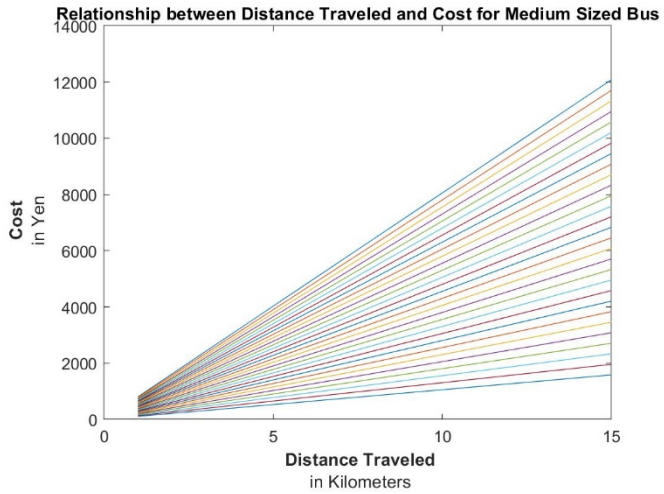

The bus routes optimization problem is a multi-objective optimization problem, multi-objective optimization problems are usually complex. To reduce the complexity of a multi-objective optimization problem, choose an objective with more importance is needed. In this section, we will discuss our analysis on the objective selection. In this network optimization problem, there are two major objective functions that needs to be optimized. One of the objective needs to maximize is the service of optimized bus network. The bus services in the Toyota city is a public transportation service, therefore as a public transportation service it needs to reach as many local residents as possible. The other objective needs to minimize is the operating cost of the service. As a public transportation service, the operating cost cannot be too high, otherwise the high cost public transportation service will be a potential tax burden of the local residents. In order to choose the better objective, we studied the relationship between the total operating cost and service coverage. We also studied the relationship between operating cost per passenger and number of passengers' bus carries.

The first study is the study of relationship between total operating cost and service coverage. For the service coverage we use 1 km – 15 km with increment of 0.1 km as the range of potential service coverage. For the total service cost, we used following equations:

$$C_{True} = C_{Total} - R_{Tickets} \quad (9)$$

$$C_{Total} = C_{Fuel} + C_{Driver} + C_{Other} \quad (10)$$

$$R_{Tickets} = N_{passenger} * D * 25 \quad (11)$$

In equation 11, the equation represents the calculation of ticket revenue. The ticket revenue is equal to the distance of travel multiply by the number of passengers and fare rate which is set by Japanese government.

The second study is the study of relationship between numbers of passengers and operating cost per passenger. This relation is also important since the population at Asahi region is relatively low.

Following plots illustrates the relationship between ridership and the operating cost for both small sized bus and medium sized bus.

Figure 3 Relationship between Distance Travelled and Operation Cost of Medium Sized Bus

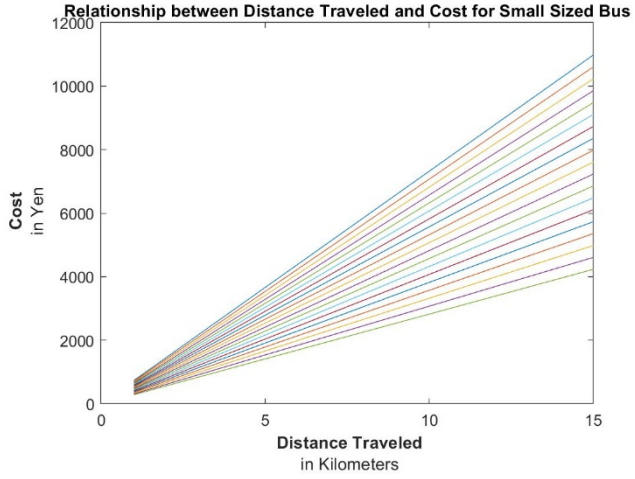

Figure 4 Relationship between Distance Travelled and Operation Cost of Small Sized Bus

From the figures above we can see a linear relationship between distance travelled and operating cost for the bus service, that means if we increase the service coverage which translates to distance travelled then the operating cost will be increase. However, the slope of this relationship differs when the numbers of passenger changes. If the passenger number increases, then the slope of this relationship decreases. Therefore if there is more passengers than the rate of increase of operating cost due to the increase of service coverage will be slower. This observation is true for both small bus scenario and medium bus scenario.

Following plots illustrates the relationship between ridership and operating cost per passenger for both small sized bus and medium sized bus.

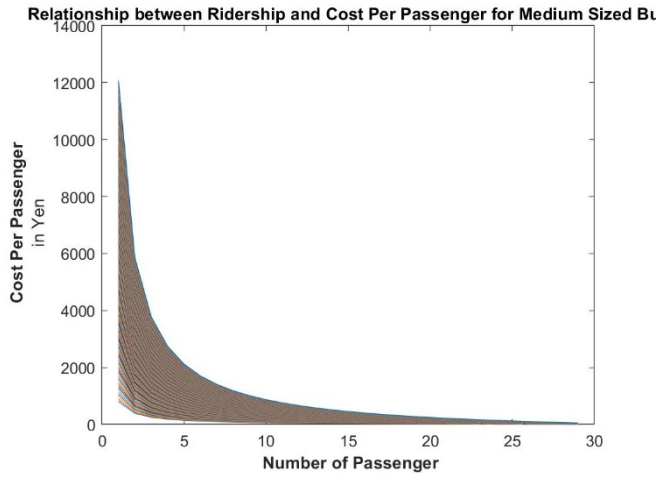

Figure 5 Relationship between numbers of passenger and operating cost per passenger for medium bus

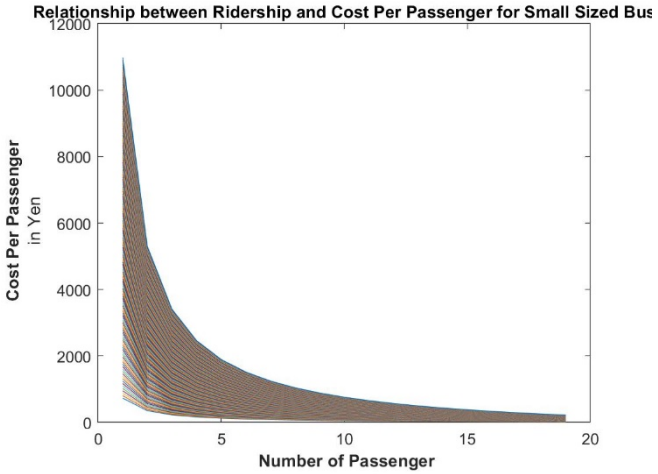

Figure 6 Relationship between numbers of passenger and operating cost per passenger for small bus

From the figures above we can see a exponential decay relationship between the ridership and operating cost per passenger. That pattern shows if we increase the ridership then the operating cost per passenger decreased exponentially. This pattern is true in both medium sized bus and small sized bus also in all of service coverage zone we analyzed. Therefore the ridership have a stronger influence on the operating cost than the service coverage.

5. PRELIMENARY SOLUTION

In the introduction and problem formulation section we discussed the combined bus route network. We used the data to calculate the total cost of the current bus network in the Asahi. In our calculation we used 1 key route trip and 2 branch route trips as the basis to find the total operating cost, the key route uses a medium size bus and branch routes use small size bus. We found out the total operating cost is around 39,000 yen. Then we combined the key route and branch routes into two combined routes, the combined routes is using the small bus. We calculated the operating cost for combined routes which equal to 30,000 yen. That represent a 22.2% of saving on just the operating cost. The main reason that combined bus network have a large cost saving is combined bus requires less driver to operate the service, for all type of the cost with in the operating cost, the cost for driver is the largest component. Therefore, reduced staffing leads to a significant cost saving. Also the combined bus network means the time saving for the passengers because the transfer is eliminated and the wait between the bus trips is zero.

6. CONCLUSION

The preliminary solution shows the optimized bus network can greatly improve the travel time between asahi and asuke. The preliminary solution also shows the operating cost of optimized bus network is reduced significantly. However, there are still a lots of the work could be done in the future to get a more optimized solution for the bus route in the asahi region. For example, due to the time constraint of this study, detailed calculation with heuristics algorithms was not possible. With expanded time frame in the future the heuristics algorithms can be applied to find a good solution. Also, in the future the work can be done on demand prediction. The demand prediction is important as it can help to allocated the best route with a full load of passengers which helps to further reduce the operating cost.

ACKNOWLEDGEMENTS

Special thanks to Miwa Sensei for provide the necessary resource for this project. Also special thanks to the TA Jiang Feng and Huang Xinyi for helping me to get familiarized with the Nagoya University and NUTREND lab.

REFERENCES

[1] Aichi Prefecture, “Statistical Data of Aichi”, 2018. [Online].Available: http://www.pref.aichi.jp/toukei/index-e.html
[2] Toyota City, “Digital Map: Toyota City Bus Map”, 2018. [Online].Available: http://michinavitoyota.jp/portal/pdf/bus/busmap_b_201804.pdf

[3] H.Taha, Operations Research. Upper Saddle River, NJ: Prentice Hall, 2007
[4] J.Yu, “Traveling Salesman Problems”, [Online]. Available: https://optimization.mccormick.northwestern.edu/index.php/Traveling_salesman_problems

Gate Leakage Based Timer Design for Biomedical Devices

Sida Li[1], Atsuki Kobayashi[2], Kiichi Niitsu[2] and Dejan Markovic[1]

Department of Electrical and Computer Engineering, University of California, Los Angeles, US

Department of Electronics, Graduate School of Engineering, Nagoya University, Nagoya, Japan

Abstract

This paper presents two gate-leakage-based timers. The first timer is a comparator based RC oscillator. To reduce the power consumption, the topology that discharges the pre-charged capacitor via a gate leaking MOS capacitor with low-leakage switch is employed. To minimize the effect of the offset of the comparator on the frequency, the three reference voltages are designed wisely. The second oscillator using an amplifier-less switching technique that can realize stable and low-voltage operation with logic circuits based architecture. To generate stable oscillation frequency in a large range of supply voltage, dynamic leakage suppression logic is adopted. The chip will be fabricated in 55-nm deeply depleted channel (DDC) CMOS technology. The simulation results achieve a power consumption of 15 and 33.3 pW at a supply voltage of 0.5 V with a body bias in a 200 um^2 area.

Keywords—Gate-leakage, low-voltage, oscillator, subthreshold, timer.

Undisclosed

CONTROLLING FLOWER STICK ROTATION USING 3D VISION FEEDBACK

Fadi A. Rafeedi

Department of Mechanical and Aerospace Engineering , Graduate School of, UCLA
frafeedi@g.ucla.edu

Supervisor: Yasuhisa Hasegawa

Graduate School of Engineering, Nagoya University
hasegawa@mein.nagoya-u.ac.jp

ABSTRACT

Flower stick juggling using a non-grasping manipulator is a dexterous task. This work focuses on generating the planar cyclic motion of the flower stick using a 3 DoF robotic manipulator with a nongrasping end effector. For this motion we develop an algorithm to achieve a stable limit cycle which the flower stick converges to. Furthermore, we design and implement a versatile environment for the robot. This environment enables us to easily adjust the camera distances and the lightning configuration. We will also introduce another position feedback of the top plane of the robot using another high-speed camera. We also design an independent controller to reject disturbances to the flower stick.

Undisclosed

EVALUATION OF GAIT STABILITY IN THE USE OF A WEARABLE WALK ASSIST DEVICE

Xuan Yang

Department of Mechanical Engineering, Graduate School of University of California, Los Angeles.

yxpegasus@g.ucla.edu

Supervisor: Prof. Yoji Yamada

Graduate School of Engineering, Nagoya University

akiyama-yasuhiro@mech.nagoya-u.ac.jp

ABSTRACT

This report demonstrates a method to evaluate gait stability of a wearable walking-assist device by using extrapolated center of mass (XCoM) concept in curving motion. The method was used to analyse gait stability from experiment data done in previous work, in which 40 trials were performed on a healthy male subject to finish a certain fixed curving trajectory using the same device. When curving the round corner, the experiment trials were divided into two groups depending on whether hip adduction/abduction and rotation were restricted or not. The results show evaluation of this curving gait stability in restricted and unrestricted out-of-sagittal plane motion.

1. INTRODUCTION

Life quality of the elderly has been a worldly heated topic nowadays. Wearable robot has been a major focus for robotic research aiming to improve daily living activities and help to prevent the unexpected accidents from happening to the elder people [1].

A recently popular robot, physical assistant robots (PARs), has been developed aiming for gait rehabilitation in hospitals and widely put into daily usage gradually. Nevertheless, PAR restricts users' out-of-sagittal motion, which decreases the efficiency to create DOF at the lower limb joint and makes it harder for the user to turn or make a curve. So this restriction may be considered as a limitation especially in curving motion to prevent its widespread usage [1]. On the other hand, however, freeing the restriction makes gait motions more complex and center of mass (CoM) move outside of base of support (BoS) easier, which may decrease the efficiency of PAR to apply assist torque and force and easily break one's balance. Therefore, it's important to analyse the gait stability in use of such kind of device with and without restriction at the hip joint.

To evaluate gait stability, there are two questions needs to be answered: (1) Balance could be maintained based on what conditions. (2) How good the balance is in a certain situation [2]. An universally acknowledged simple mechanical model for human standing is the inverted pendulum. The projection of CoM should be controlled inside of BoS. But in walking situation, taking velocity of CoM into account is necessary [3]. In dynamic situation, there are several measures which also consider velocity of CoM to analyse gait stability, such as the extrapolated center of mass (XCoM) by Hof *et al*, foot placement estimator (FPE) by Millard *et al* and stabilizing and destabilizing forces by Duclos *et al* [3]. Since XCoM concept is famous for analysing gait stability based on experiment data and more robust among those three, it's used here to compare gait stability using the wearable walking-assist robot between restricted condition and unrestricted condition.

2. METHOD

This report uses XCoM concept to analyze gait stability from experimental data in a certain known curving motion. To calculate stability index, local coordinates are formed in two different ways: cartesian method and polar method, which will be illustrated in detail in part **2.4**.

2.1 Curving Experiment

In the previous work, forty experiments were performed on a healthy male subject to walk along a certain known curving trajectory (Shown in Fig.1). It consists of a quarter arc with 0.5 m radius and two straight lines. The subject was asked to walk along the trajectory wearing the walking-assist device (Shown in Fig.2) and the zoomed part is used to switch between restricted condition and unrestricted condition. As shown in Fig.1, four steps were recorded using a Motion Analysis Corporation system (MAC 3D system, U.S.) and the second gait cycle consisted of 2nd, 3rd, 4th steps will be mainly focused on. The position of CoM, foot heels, foot toes and four corner points of pelvis in x-y-z axis were recorded by attaching markers of the SIMM Motion Module (SIMM, Mulsculographics Inc, U.S.) to better fit human model. Force plates and force sensors (M3D, Tech Gihan Co, Ltd, Japan) were attached to each foot heel and foot toe to record ground reaction force so that the timing of gait events could be detected [1].

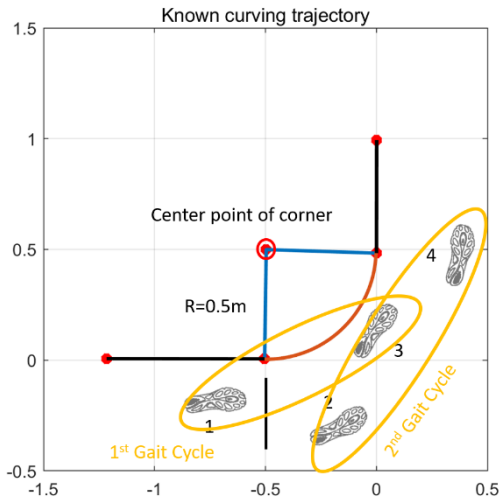

Fig.1 Known curving trajectory and steps.

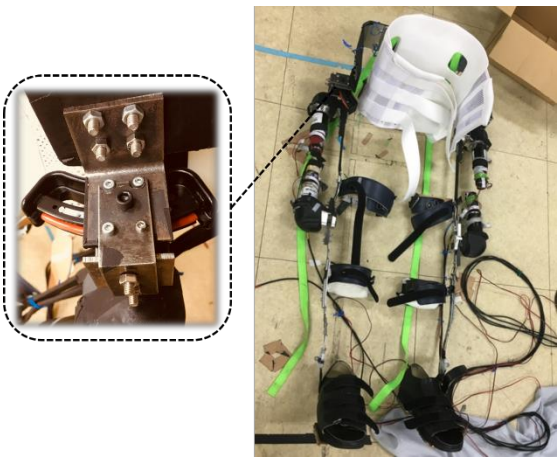

Fig.2 Wearable walking-assist device and the part to control restricted or unrestricted condition.

Each trial lasted for about 2.5 s, and the data recording interval is 0.01 s. In the following analysis, the first step using left foot (inner foot) will be separated from the first step with right foot (outer foot). Among those 40 experiments, 20 of them were in unrestricted condition, which means the subject could move or rotate the hip joint freely during curving motion. On the contrary, the other 20 experiments were carried out in restricted condition, which means the hip joint lost DOF in out-of-sagittal direction and rotation but could only move inside of sagittal plane.

2.2 XCoM Concept

According to Hof *et al*, the inverted pendulum human model is used, in which the mass of the body is regarded as a single point mass supported by a massless leg [4]. Applying this assumption to unperturbed walking, the main parameters needed to be calculated are defined as the following:

$$\mathbf{XCoM} = \mathbf{CoM} + \frac{\mathbf{V}_{CoM}}{\omega_0} \tag{1}$$

$$\omega_0 = \sqrt{\frac{g}{l}} \tag{2}$$

$$\mathbf{b} = \mathbf{BoS} - \mathbf{XCoM} \tag{3}$$

in which **XCoM** is the extrapolated center of mass. **CoM** is center of mass. $\mathbf{V}_{CoM}$ denotes velocity of center of mass. And ω_0 is the inverted pendulum's eigen-frequency defined as square root of acceleration of gravity (9.8 m/s^{-2}) divided by length of pendulum. **b** is the margin of stability defined as the distance between base of support (**BoS**) and **XCoM** [3]. And bold font variables here denote vectors in x-y plane.

This method shows the extent of closeness that the human model is about to fall. The smallest b denotes the most unstable point within a step. When b is negative, it means XCoM has already passed BoS, in which case adaptive actions may be required such as one more step or adjustment from arms or other body part [3].

2.3 Critical Parameters

To calculate temporal stability of margin and extrapolated center of mass during curving motion, the position of CoM of the whole body and BoS at each time point need to be known timely. And some other key parameters need to be defined and calculated.

2.3.1 Velocity of CoM

Velocity of CoM was calculated from the position of CoM using the following equation:

$$\mathbf{V}_{CoM_k} = \frac{\mathbf{V}_{CoM_{k+1}} - \mathbf{V}_{CoM_{k-1}}}{0.02} \tag{4}$$

in which k means the k-th recording time point. And 0.02 is two times of the data recording interval.

2.3.2 Pendulum Length

Pendulum length was chosen from the maximum height of CoM in each trial and mean value of all trials. It's calculated separately in restricted and unrestricted condition. For restricted condition, pendulum length is 0.97 m. And it's 0.98 m in unrestricted condition.

2.3.3 Base of Support

To define BoS, the ground reaction forces are needed. When the reaction force is above the force threshold (10 N), then it will be regarded as sufficiently contacting with ground (Shown in Fig.3).

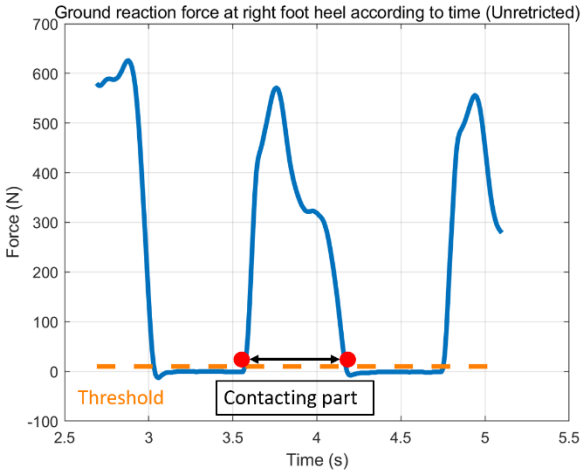

Fig.3 Ground reaction force of right foot heel and ground contacting part.

The ground reaction force of heel and toe of each foot was detected and recorded in the experiment data. The heel marker (containing the radius of the marker) is the demarcation on the posterior boundary of the foot, while the toe marker is on the distal border of toes [5]. BoS is defined based on the ground contacting part. In each gait cycle, both stance phase (with two feet contacting with ground) and swing phase (with only one foot contacting with ground), whose BoS is quite different from each other, are included (Shown in Fig.4). When there is only one foot stepping on the ground, BoS is consisted of four corner points (r1, r2, r3, r4) on the boundary of the foot calculated from the measured width of toes and heel vertical to heel-to-toe vector. In double feet support situation, BoS is defined as the area within the minimum and maximum position of 8 corner points (L1, L2, L3, L4, R1, R2, R3, R4) on the foot boundary calculated using the same method as stance phase condition in x and y direction respectively, expressed in local coordinate which will be illustrated in detail in part **2.4**. And the four boundaries of BoS is parallel to x, y axis of the local coordinate.

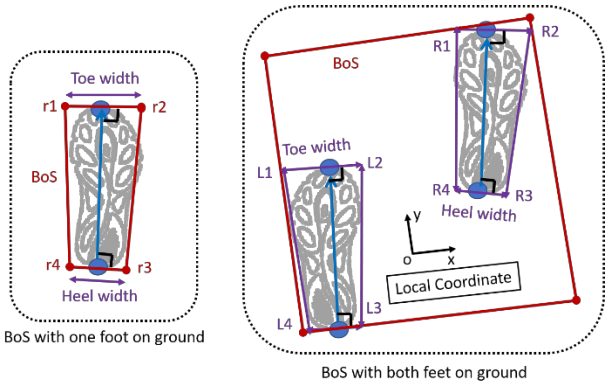

Fig.4 Definition of BoS in single foot supporting condition and double feet supporting condition.

2.3.4 Margin of Stability

Margin of stability is calculated using equation (3). In forward position (along y direction), since XCoM is always near maximum BoS comparing to minimum BoS. So b_y is calculated by the following equation (5):

$$b_y = (\max)BoS_y - XCoM_y \tag{5}$$

So margin of stability here in y direction is defined as vertical distance between the upper boundary of BoS and XCoM (as shown in Fig.5). For lateral position (along x direction), however, the distance between BoS and XCoM is largely influenced by velocity of CoM. To analyse gait stability more effectively, margin of stability in x direction is defined as:

$$b_x = \begin{cases} (\max)BoS_x - XCoM_x & V_{CoM_x} > 0 \\ XCoM_x - (\min)BoS_x & V_{CoM_x} < 0 \end{cases} \tag{6}$$

in which the maximum BoS is the right boundary of BoS and minimum BoS is the left boundary of BoS expressed in local coordinate. When the velocity of CoM is positive, which means the CoM of the subject was about to move towards maximum BoS, the parallel distance between right boundary BoS and XCoM will be calculated since the gait stability may be the most vulnerable in this direction (see Fig.5). Similarly, when the subject was moving towards negative x direction, the distance between left boundary of BoS and XCoM will be calculated as margin of stability.

Since the safe and stable area is within the BoS, the larger distance XCoM is from each boundary of BoS, meaning larger margin of stability, more stable the gait becomes.

2.4 Local Coordinate

Gait stability is analysed in timely defined local coordinates. Here two methods were used, cartesian method

and polar method. Then using homogeneous matrix to transfer the position of each key point to the local coordinate.

2.4.1 Cartesian Method

In Fig.5, the isosceles trapezoid represents pelvis of the subject. The origin of the local coordinate is defined as the center of the pelvis. Four points on the corner of the pelvis, L.ASIS, R.ASIS, L.PSIS, R.PSIS are left and right side of pelvis in the front together with left and right side of pelvis at the back respectively. Local x axis is parallel to the front line of the pelvis, while y axis is vertical to it. The unit vector in x direction is calculated from normalized vector pointing from L.ASIS to R.ASIS, denoted as $[X_x \quad X_y]^T$. Rotating x unit vector $90°$ to the left, unit vector in y direction will be attained, denoted as $[Y_x \quad Y_y]^T$.

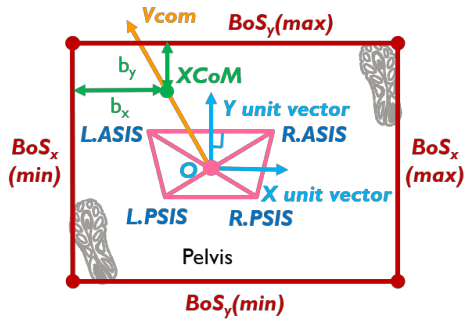

Fig.5 Definition of local coordinate in Cartesian method.

2.4.2 Polar Method

In this method, curving motion trajectory is needed to define the polar coordinate. The global origin expressed in polar coordinate should be located at the center of each curving motion. Since it was impossible for the subject to exactly follow the given curving trajectory in each trial, the walking data of position of CoM is needed to find out the motion circle which could perfectly fit the real curving motion (Shown in Fig.6). To define the local coordinate, first move the global origin to the center of the fitted motion circle. Then define the position of CoM expressed in current coordinate as the local origin and transfer it to polar coordinate, denoted as (θ_0, ρ_0). Let the direction along radius to be the local x axis, while y axis is defined as the tangent direction to the fitted motion circle (Shown in Fig.7). In this way, the unit x vector could be formed by using point CoM and point $(\theta_0, \rho_0 + 1)$, and then rotate it by $90°$ to form the unit y vector.

As stated in last paragraph, since the real motion trajectory varies between each trial, the fitted circle including the location of center and radius is different from each trial (Shown in Fig.8). This has become an additional influence factor to results. Thus, in the following analysis, Cartesian method will be applied.

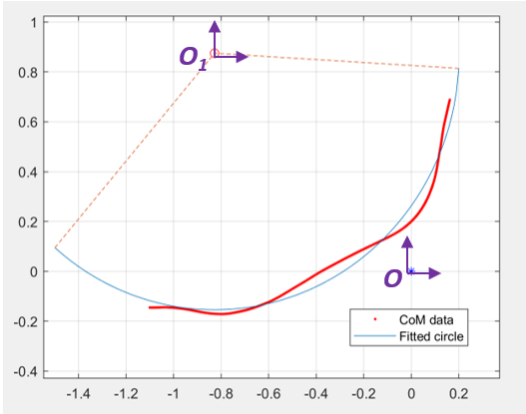

Fig.6 Finding out the fitted motion circle using real CoM motion trajectory.

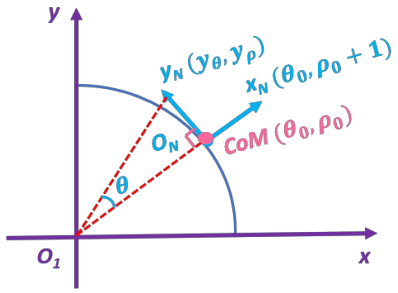

Fig.7 Definition of local coordinate in polar method.

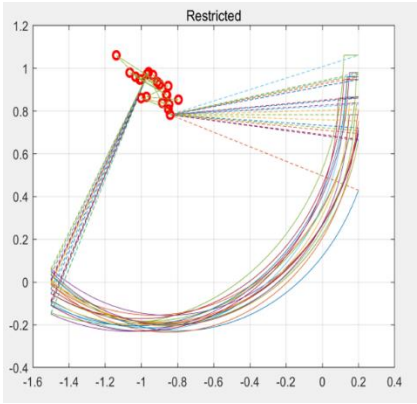

Fig.8 Fitted motion circle of all trials in restricted condition.

3. RESULTS

The margin of stability of the second gait cycle in each direction was calculated at each time point. The 2nd, 3rd and 4th step, which is at the time point just before each heel contact, has been further analyzed.

3.1 Forward Stability

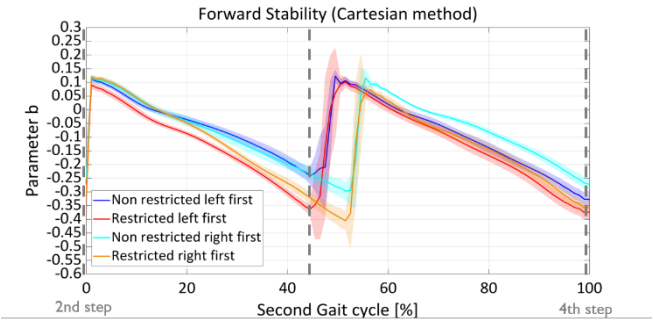

Fig.9 Margin of stability during the 2nd cycle in y direction.

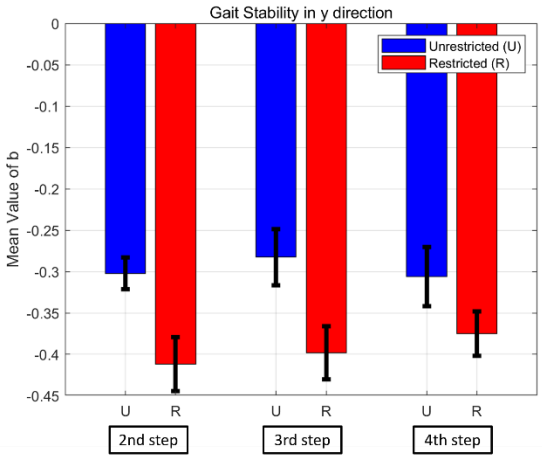

Fig.10 Mean value and standard deviation of margin of stability at 2nd, 3rd, 4th step in y direction.

From Fig.9, the most unstable situation where the margin of stability is relatively small happens at the time just before the heel contact of each step. So the mean value and standard deviation of margin of stability is analyzed individually in Fig.10. Each bar is the mean value, where the black error bar shows standard deviation.

From the mean value in Fig.10, it's obvious that unrestricted condition works better than restricted condition in y direction.

3.2 Lateral Stability

Fig.11 and Fig.12 also shows the most unstable situation happens at each step. But the margin of stability in x direction of all trials are not consistent. They vary a lot between each trial. Especially at the third step, for example, for some of the cases, the margin of stability stays high, while the others jump down to negative value. Therefore, further analysis is needed here.

Fig.15 shows that margin of stability jumps when the velocity of CoM changes its sign. And Fig.16 shows that the velocity of CoM is very different in each trial instead of coinciding. Some of the trials at the third step, velocity of CoM still stays positive, which means the subject failed to change direction at this time, while the velocity in other cases become negative. And those positive cases only happen in restricted condition, which will be omitted from the further analysis at each step. This phenomenon may reflect that the restricted condition makes it harder for the subject to change direction in time.

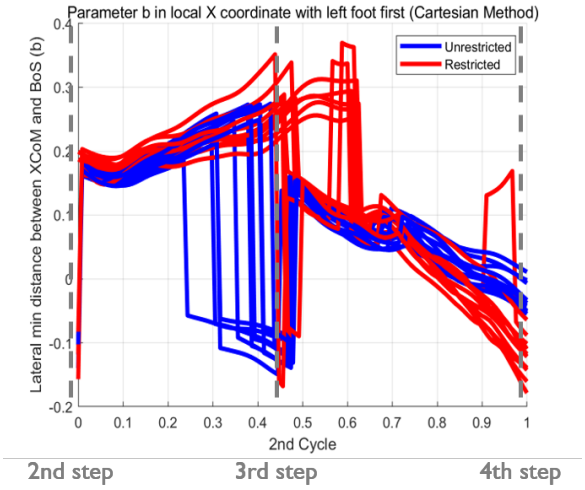

Fig.11 Margin of stability during the 2nd cycle in x direction when the first step is left foot.

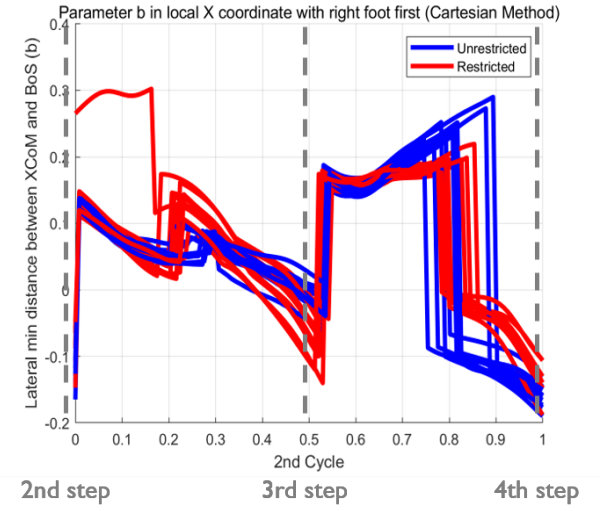

Fig.12 Margin of stability during the 2nd cycle in x direction when the first step is right foot.

From Fig.13 and Fig. 14, it illustrates that unrestricted condition is only more stable on right foot (outer foot in curving motion). And the standard deviation of unrestricted condition is smaller than restricted condition, which means

the gait cycle in unrestricted condition is more stable and robust.

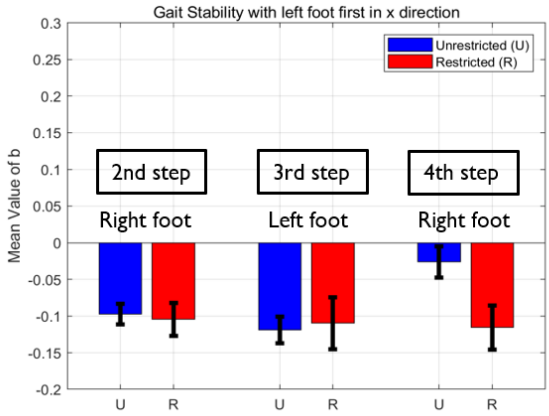

Fig.13 Mean value and standard deviation of margin of stability at 2nd, 3rd, 4th step in x direction only for the cases when the first step is left foot.

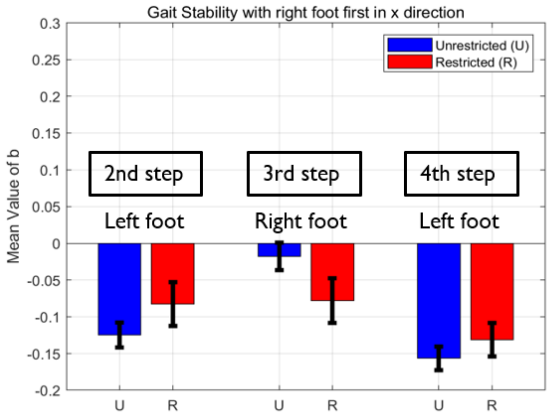

Fig.14 Mean value and standard deviation of margin of stability at 2nd, 3rd, 4th step in x direction only for the cases when the first step is right foot.

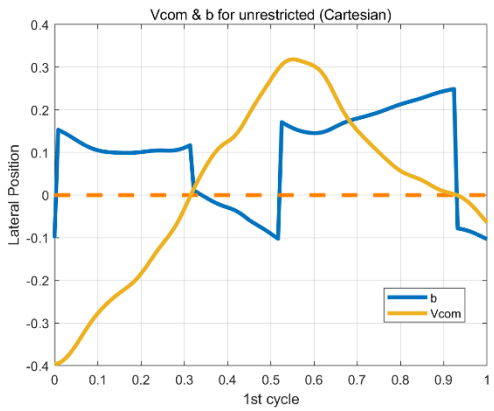

Fig.15 Relationship between velocity of CoM and margin of stability in x direction.

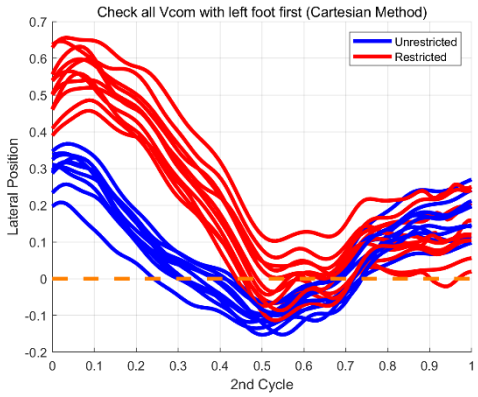

Fig.16 Velocity of CoM of all trials.

4. SUMMARY

In this report, XCoM concept has been performed to analyze walking gait stability in the use of a wearable walking-assist device during curving motion. The gait stability has been compared between both conditions whether the hip joint was restricted or not while curving by estimating the margin of stability. Moreover, how the curving gait stability being influenced by restricted condition has been further analyzed.

The results show that the restricted condition is less stable in forward position. It may also prevent the user from changing direction in time while curving. Gait cycle is easily perturbed in restricted condition. For lateral position, restricted condition seems more stable on the inner foot and less stable on the outer foot in curving motion.

ACKNOWLEDGEMENTS

Thanks to Prof. Yamada for giving me the previous opportunity to come to Japan and join Yamada Lab doing interesting research during this summer vacation. Thanks to Prof. Akiyama for great help and guidance on my research. Special thanks to my TA Kuboki, my lab friend Guanqun Yang for their kind help and advice. I'd also like to thank all the lab mates for the unforgettable summer memory we created together.

REFERENCES

[1] Fukui Y, Akiyama Y, Yamada Y, et al. The change of gait motion when curving a corner owing to the motion restriction caused by a wearable device[C]//Systems, Man, and Cybernetics (SMC), 2017 IEEE International Conference on. IEEE, 2017: 525-530.

[2] Hof A L, Gazendam M G J, Sinke W E. The condition for dynamic stability[J]. Journal of biomechanics, 2005, 38(1): 1-8.

[3] Bruijn S M, Meijer O G, Beek P J, et al. Assessing the stability of human locomotion: a review of current measures[J]. Journal of the Royal Society Interface, 2013, 10(83): 20120999.

[4] Hof A L. The ‘extrapolated center of mass’ concept suggests a simple control of balance in walking[J]. Human movement science, 2008, 27(1): 112-125.

[5] Lugade V, Lin V, Chou L S. Center of mass and base of support interaction during gait[J]. Gait & posture, 2011, 33(3): 406-411.

JUACEP Indenpedent Research Report
Nagoya University, Japan

A Study on Autonomous Motion Planning of Mobile Robot by Use of Deep Reinforcement Learning for Fall Prevention in Hospital

Guanqun Yang

Department of Electrical and Computer Engineering, University of California, Los Angeles
guanqun.yang@engineering.ucla.edu

Supervisor: Yoji Yamada

Graduate School of Engineering, Nagoya Universitys
yoji-yamada@mech.nagoya-u.ac.jp

ABSTRACT

The number and severity of elderly-involved accidents, especially falls, have posed great challenge to this aging society. Economical in cost and versatile in ability, mobile robots' role could not be neglected in elderly care service. In this paper, we put forward a novel architecture of autonomous motion planning which integrates object detection and reinforcement learning. This architecture makes possible secure path generation from environment prone to danger factors to elderly population in real time. Simulation results provides a visualization of each component and indicates effectiveness of this system.

1 INTRODUCTION

The United Nations data indicates that the number of elderly people could exceed 2.1 billion in 2050 and 3.1 billion in 2100 with growth rate higher than that of all other age groups [1]. At the same time, two tendencies are observed by academic community regarding aging population. One is the number of elderly-involved accidents, especially unexpected falls, is growing rapidly and could cause as many as 7 mortalities every single hour in United States by 2030 [2]. Another one is the steady increase of elderly-care service, which on average costs $6844 for a single month in United States each person [3].

Meanwhile, the versatility and cost-efficiency of mobile robots also draw researchers' attention. With their participation in elderly care service, the number of accidents and cost of service are expected to be considerably reduced. Furthermore, the novel deep learning and reinforcement learning theory could be directly applied to elderly care service through their implementation on these robotics platforms.

In this work, we present an architecture that detects safety route autonomously in hospital setting with mobile robots through deep reinforcement learning. This paper is organized as follows: part 1 shows the challenge and potential solution people have in elderly care service; part 2 provides an overview of our system through algorithmic diagram; part 3 shows the process we acquire the application-specific dataset; part 4 and part 5 briefly introduces ideas underlying and provides experimental results and corresponding evaluations.

2 SYSTEM ARCHITECTURE

From the introduction in part 1, the major objects of fall prevention is two-fold:

1. Detect a secure route from indoor map through deep reinforcement learning
2. Lead the user to his or her destination according to the route detected in step 1

The task in step 2 is largely a solved problem with multiple working implementations [4, 5]. Therefore, we mainly focus on step 1.

As is seen from the algorithm 1, when fed into the map of environment, the mobile robot continuously explore the entire environment and makes safety spot annotation or danger spot annotation through deep learning-based object detection and danger level evaluation. When all blocks are annotated, path planning based on reinforcement learning is enacted and thereby a safety route. Note multiple routes are possible after route detection so path could chosen by user based on their preferences.

3 DATASET PREPARATION

Preparing an dataset immediately related to our hospital scene setting is the requisite for utilizing out-of-state object detection

Result: Secure Path
Input: Environment Map
while *map not fully explored* **do**
  exploring environment and detecting dangers;
  if *danger detected* **then**
    DangerLevel = DangerEvaluation();
    DangerSpotAnnotation(DangerLevel);
  else
    SafetySpotAnnotation();
  end
end
SecurePath = MotionPlanning();

Algorithm 1: Process of Secure Route Detection

Figure 1: The Hospital Scene Dataset With 29 Categories

framework for danger factor detection. However, to our best knowledge, such dataset is not available even though there does exist some datasets regarding surgery process and other medical activities where specific operations to patients are recorded [6, 7]. Our best hope is that common danger factors in hospitals and elderly care facilities could be included in our dataset.

By combining famous Places205 dataset and public domain Google image search results and after dataset preparation procedures described in algorithm 2[8], the dataset with 29 categories of danger factors is extracted. As is shown in Table 3, the number of each category of images is 100 and the image size is 256×256, which is suitable for the fine-tuning of convolution neural network. A snapshot of this dataset is shown in Figure 1.

Table 1: Statistics of Dataset

Number of Categories	Number of Images	Image Size
29	2900	256×256

Result: Hospital Scene Dataset
Input: CategoryList, Places205 Dataset, Google Search Results
for $k = 1 : ImageCount$ **do**
  category = IdentifyingCategory(image);
  if $category \in CategoryList$ **then**
    labeling image with category identifier $(1, 2, \cdots, 29)$
  else
    lebeling image with 0;
  end
end
for $k = 1 : ImageCount$ **do**
  automatic resizing;
  automatic categorization with category identifier;
end

Algorithm 2: Procedures of Dataset Preparation

4 OBJECT DETECTION

YOLO is a object detection implementation that outperforms others regarding speed with comparable mean average precision (mAP). As is shown in Table 2, the platform could process video stream with as many as 91 frames per second (FPS) [9, 10, 11].

Table 2: Comparison of Out-of-State Object Detection Platform

Detection Framework	mAP	FPS
Fast R-CNN	70.0	0.5
Faster R-CNN ResNet	76.4	5
Faster R-CNN VGG-16	73.2	7
SSD300	74.3	46
SSD500	76.8	19
YOLO 256×256	69.0	91

However, the YOLO was original trained on PASCAL VOC 2007 dataset with limited number of categories [12]. Therefore, the fine-tuning of convolutional neural network (CNN) used in YOLO system is required.

Table 3: Categories in PASCAL VOC 2007 Dataset

Type	Category
Person	person
Animal	bird, cat, cow, dog, horse, sheep
Vehicle	aeroplane, bicycle, boat, bus, car, motorbike, train
Indoor	bottle, chair, dining table, potted plant, sofa, tv/monitor

Since our dataset is small and different from the PASCAL VOC 2007 dataset the YOLO was originally trained on, the fine-tuning of the network is allowed. Specifically, only layers that extract lower-level features including lines, arcs and circles are kept and the resulting network is trained on our dataset with linear classifier as output.

As is shown in Figure 2, the fine-tuned network could detect bed, which is previously unavailable.

Figure 2: Result of Fine-Tuned YOLO Detection System

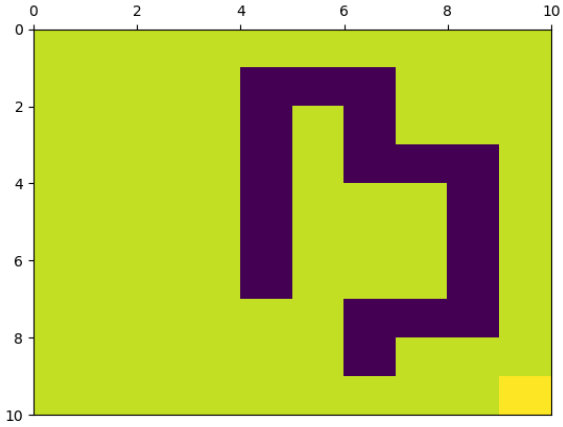

Figure 3: Simulation Setting

5 MOTION PLANNING

Reinforcement learning is a process that enables agent to learn a sequence of actions through interaction with environment in a trial and error fashion. It could be formalized as a Markov decision process (MDP) and parameterized as a tuple $\langle S, A, P, R, s_0 \rangle$ [13]. Specifically, S is the state set where the agent could transition to; A is the action set including a list of allowable actions that could be taken by agent; $P(s_{t+1}|s_t, a_t)$ is the system dynamic that describes the probability of making transition from s_t to s_{t+1} by taking action $s_t \in S$; and $R(s_{t+1}|s_t, a_t)$ is the reward of making such transition.

The solution to the MDP could be described in algorithm 3, which is a dynamic programming-based approach. At each iteration, the agent chooses the action that generates most reward until there are no more rewards could be exploited from environment.

Result: Optimal action $\pi(s)$ at each state s
for $k = 1 : \infty$ **do**
  $V_k[s] = \max_a \sum_{s'} P(s'|s,a)R(s\prime|s,a) + \gamma V_{k-1}[s']$;
  if $\forall s, |V_k(s) - V_{k-1}(s)| < \epsilon$ **then**
    $\pi(s) =$
    $\text{argmax}_a \sum_{s'} P(s'|s,a)R(s\prime|s,a) + \gamma V_{k-1}[s']$;
  end
end

Algorithm 3: Algorithm to Solve MDP

In one complicated setting shown in Figure 3, where dark areas represent danger spots and bright area in down-right corner represent destination, the mobile robot could autonomously decide optimal action in each state, as is shown in Figure 4. More detailedly, the mobile robot tries to avoid the danger spots and the actions taken near these areas are all going down.

Based on the result provided by Figure 4, a secure route could be detected and the autonomous motion planning is made possible.

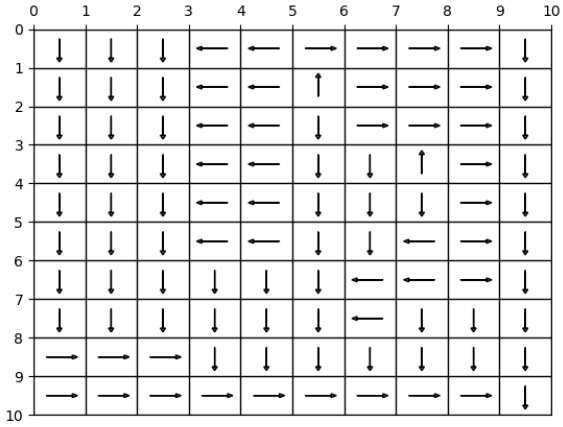

Figure 4: Simulation Result

6 CONCLUSION

In this work we put forward a novel architecture for secure route generation in the background of fall prevention in hospital or other elderly care facilities through deep reinforcement learning. A hospital scene dataset is first created to suit our purpose that applying our system in hospital setting. Then fine-tuned object detection system allows real time danger factor detection from live video stream. Finally, the reinforcement learning-based motion planning module makes possible the secure route generation in complicated hospital setting.

At the same time, we notice that the number of danger factors is still lacking when attempting to apply the system in real world. Therefore, more categories of images should be collected and added to our dataset. Additionally, the system integration of indoor mapping, object detection and motion planning is largely still a undone task and may involve numerous practical implementation issues. In the future, our work will continue in both of the two aspects.

ACKNOWLEDGEMENT

This work could not be made possible without the support coming from multiple sources. First we appreciate the JUACEP program and its coordination with several renowned institutions, including UCLA, in north America. The program and international cooperation is the requisite for this research experience. Then this work would be otherwise difficult, if not impossible, to complete in a smooth fashion without the invaluable support from Yamada lab, where Mr. Takaaki Namba, Mr. Eugene Kim and Prof. Yoji Yamada provides timely guidance in not only theoretical aspect but experimental aspect as well. Eventually, the generous financial support provided by JASSO guarantees a memorable research experience in Japan.

REFERENCES

[1] United Nations. World population prospects: The 2017 revision. *United Nations Econ Soc Aff*, 33(2):1–66, 2017.

[2] Centers for Disease Control and Prevention. Important facts about falls, 2016.

[3] Depart of Health and Human Services. Costs of care, 2016.

[4] Sebastian Thrun, Maren Bennewitz, Wolfram Burgard, Armin B Cremers, Frank Dellaert, Dieter Fox, Dirk Hahnel, Charles Rosenberg, Nicholas Roy, Jamieson Schulte, et al. Minerva: A second-generation museum tour-guide robot. In *Robotics and automation, 1999. Proceedings. 1999 IEEE international conference on*, volume 3. IEEE, 1999.

[5] Takayuki Kanda, Masahiro Shiomi, Zenta Miyashita, Hiroshi Ishiguro, and Norihiro Hagita. An affective guide robot in a shopping mall. In *Proceedings of the 4th ACM/IEEE international conference on Human robot interaction*, pages 173–180. ACM, 2009.

[6] Andru P Twinanda, Sherif Shehata, Didier Mutter, Jacques Marescaux, Michel De Mathelin, and Nicolas Padoy. Endonet: A deep architecture for recognition tasks on laparoscopic videos. *IEEE transactions on medical imaging*, 36(1):86–97, 2017.

[7] Ralf Stauder, Daniel Ostler, Michael Kranzfelder, Sebastian Koller, Hubertus Feußner, and Nassir Navab. The tum lapchole dataset for the m2cai 2016 workflow challenge. *arXiv preprint arXiv:1610.09278*, 2016.

[8] Bolei Zhou, Agata Lapedriza, Jianxiong Xiao, Antonio Torralba, and Aude Oliva. Learning deep features for scene recognition using places database. In *Advances in neural information processing systems*, pages 487–495, 2014.

[9] Joseph Redmon, Santosh Divvala, Ross Girshick, and Ali Farhadi. You only look once: Unified, real-time object detection. In *Proceedings of the IEEE conference on computer vision and pattern recognition*, pages 779–788, 2016.

[10] Joseph Redmon and Ali Farhadi. Yolo9000: better, faster, stronger. *arXiv preprint*, 2017.

[11] Joseph Redmon and Ali Farhadi. Yolov3: An incremental improvement. *arXiv preprint arXiv:1804.02767*, 2018.

[12] M. Everingham, L. Van Gool, C. K. I. Williams, J. Winn, and A. Zisserman. The pascal visual object classes (voc) challenge. *International Journal of Computer Vision*, 88(2):303–338, June 2010.

[13] Seyed Sajad Mousavi, Michael Schukat, and Enda Howley. Deep reinforcement learning: an overview. In *Proceedings of SAI Intelligent Systems Conference*, pages 426–440. Springer, 2016.

ALUMINUM INDUCED CRYSTALLIZATION OF SILICON THIN FILM ON STRONTIUM TITANATE SUBSTRATE

Chenhui Zhou

Department of Materials Science and Engineering, Graduate School of Engineering, UCLA
zhouch1220@gmail.com

Supervisor: Prof. Noritaka Usami & Dr. Mel F. Hainey Jr.

Graduate School of Engineering, Nagoya University
usa@material.nagoya-u.ac.jp & melhaineyjr@numse.nagoya-u.ac.jp

ABSTRACT

(100) Si is the primary substrate in CMOS processing device. In previous aluminium induced crystallization (AIC) of Si on glass experiment, 95% (111) Si was grown in the thin film regime (t_{Al} < 50 nm), and 80% (100) Si was grown in the thicker film regime (t_{Al} > 50 nm).[1] In this experiment, Si on $SrTiO_3$ was selected to research on solid state heteroepitaxial growth. Because in AIC processing, Si atoms nucleate on the Al/STO interface in the thin film regime, and (100) Si and (100) STO are lattice matched, hence a more optimized (100) Si thin film was expected to be produced on STO substrate. But (111) Si film was found to be grown on (100) STO substrate when AIC was performed in the thin film regime (t_{Al} < 50 nm), and random orientated Si was grown in the thick film regime.

In the case of homoepitaxy where AIC Si grew on (100) Si, only (100) Si was produced on (100) Si substrate in the thin film regime. It was because in homoepitaxy, (100) Si on (100) Si has the perfect lattice match and the lowest interface energy. Hence the reason why (111) Si grew on (100) STO could be the energy level of (111) Si growth was lower than the energy of (100) Si/STO lattice matched growth.

AIC Si on glass in the thin film regime gave the same results that (111) Si grew on amorphous glass when t_{Al}<50nm, and random orientated Si grew on glass when t_{Al}>50nm. Glass is amorphous and lattice match does not influence the Si thin film growth. The similar results of AIC Si on STO and AIC Si on glass showed (111) Si thin film may be produced on other different substrates in the thin film regime because substrates have minimal effect of Si crystallization.

1. INTRODUCTION

Si has diamond crystal structure and STO has perovskite structure. The lattice constant of a 1*1 surface cell of (100) Si is 3.84 Å, which is very close to 3.905 Å of cubic STO. Hence (100) Si thin film was expected to heteroepitaxial grow on (100) STO substrate.

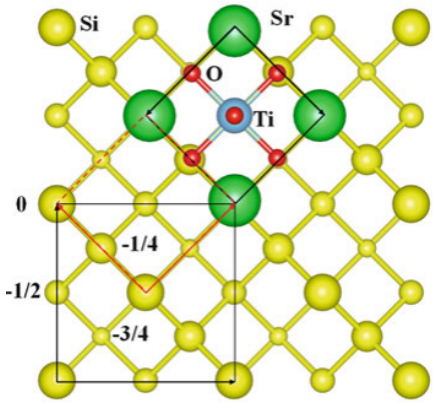

Fig. 1 Epitaxial matching of STO and Si (001)

Aluminium-induced Crystallization (AIC) is a method of growing controlled orientated high quality polycrystalline Si on different substrates. It can be operated at a low temperature around 400 ℃ to 500 ℃ that is below the eutectic point of Al/Si and softening point of substrate. And aluminium is generally cheaper than using other metal materials.

From the results of *Kurosawa et al*. group, in Fig. 2, In Group C where AIC Si grew on glass, 95% (111) Si grew on Al/SiO_2 interface when aluminum layer thickness was less than 50nm, because the minimum interface energy of (111)Si/SiO_2 is 0.9 eV/atom which was much smaller than the minimum interface energy of (001)Si/a-Al_2O_3 (3 eV/atom), and Si atoms could diffuse through the thin Al layer to nucleate on Al/SiO_2 interface.[1]

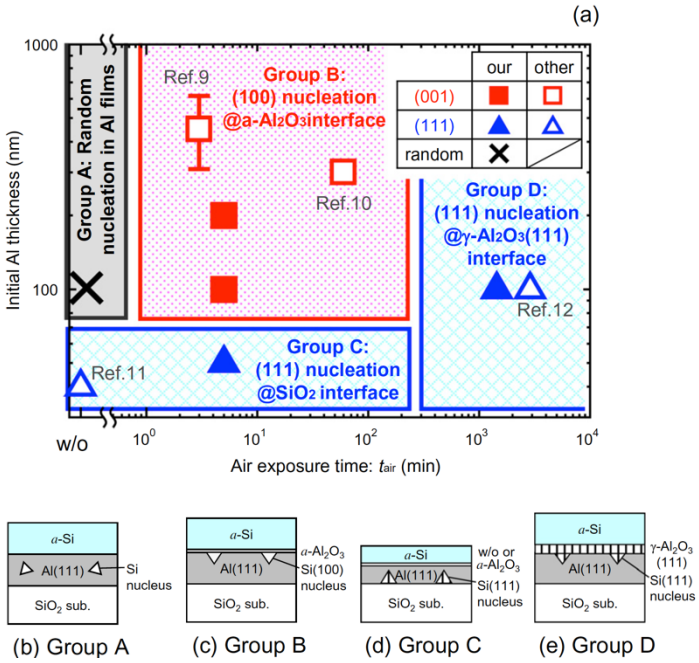

Fig. 2 (a) AIC Si orientation map, air exposure time and initial Al thickness t_{Al} dependent (b)-(e) model for preferential Si nucleation for Group A-D

The project was expecting to produce highly orientated (100) Si thin film on (100) STO substrate in the thin film regime (Group C), where Si atoms nucleate and can heteroepitaxial grow (100) Si on Al/STO interface since (100) Si and (100) STO are lattice matched.

2. EXPERIMENTAL PROCEDURE

The (100) $SrTiO_3$ (size □15(±0.1)*0.5t(±0.05)) was used as substrate. The STO piece was immersed in buffered NH_4F-HF solution (pH=4.5) for 10 minutes to remove excess oxidants on the surface, and exhibited atomically flat steps for Si crystallization.[2] Then the STO was put in IPA and distilled water for 10 minutes each ultrasonic cleaning, and rinsed in distilled water for 5 minutes, dried in a nitrogen stream. The substrate was loaded into the chamber of the RF sputtering system immediately to allow minimum air exposure.

The chamber was pumped to $2*10^{-4}$ pa in preparation of aluminum deposition. Overnight. Aluminum was sputtered onto STO substrate at 110 W RF power for 300 seconds. A 33nm thickness Al film was grew with 1.1 Å per second growth rate. For thick AIC film, sputtering time was 900 seconds, and 99 nm Al film was grew. Then chamber was opened and sample was exposed to air for 3 minutes to grow about 5 nm aluminum oxide film. Then chamber was pumped to $2*10^{-4}$ pa again to sputter amorphous silicon. Around 36 nm thickness a-Si was deposited in 450 seconds with 0.8 Å per second growth rate. For thick AIC film, sputtering time was 1200 seconds, and 96 nm a-Si film was grown. A structure of a-Si/Al_2O_3/Al/STO sample was prepared.

Sample was then annealed at T_a=450 ℃ for 4 hours or T_a=500 ℃ for 2 hours in a 0.5 sccm Argon flow. Under such t_{Al} <50nm thin film regime, Si was expected to diffuse through Al_2O_3 and Al layers, and nucleate on the Al/STO interface to form (100) poly Si layer. The existence of Al_2O_3 promoted Si atoms to nucleate on Al/STO interface rather than random nucleation.[1] After annealing was done, top Al layer was etched by immersing the sample in diluted 5% HF solution for 30 seconds. Sample was rinsed in water and dried in a nitrogen stream. In the end (100) Si thin film on STO should be prepared.

The Si grains of the sample was characterized using SEM of 15 kV acceleration voltage. The composition, grain orientation and in-plane orientation were characterized using XRD theta/2theta scan, and EBSD scan at 1000x magnification and 0.7 μm step size.

3. RESULTS AND DISCUSSION

The buffered NH_4F-HF (BHF) solution indeed improved surface smoothness of STO substrate as suggested by *Kawasaki et al.*.[2] Using atomic force microscopy, BHF pretreated STO surface exhibited atomically flat terraces (RMS roughness: 0.06 nm).

AIC on STO process behavior at different annealing temperature was examined. Sample annealed at 450 ℃ was found to have average larger size and more coalescent grains than the sample annealed at 500 ℃. The complete AIC interlayers exchange process was done within around 15 minutes. Comparing to previous study of AIC on glass by *Hainey Jr. et al.*, the layers exchange was done in around 20 minutes for AIC on glass in the thin film regime.[4] The crystallization rates for AIC on STO and AIC on glass are similar.

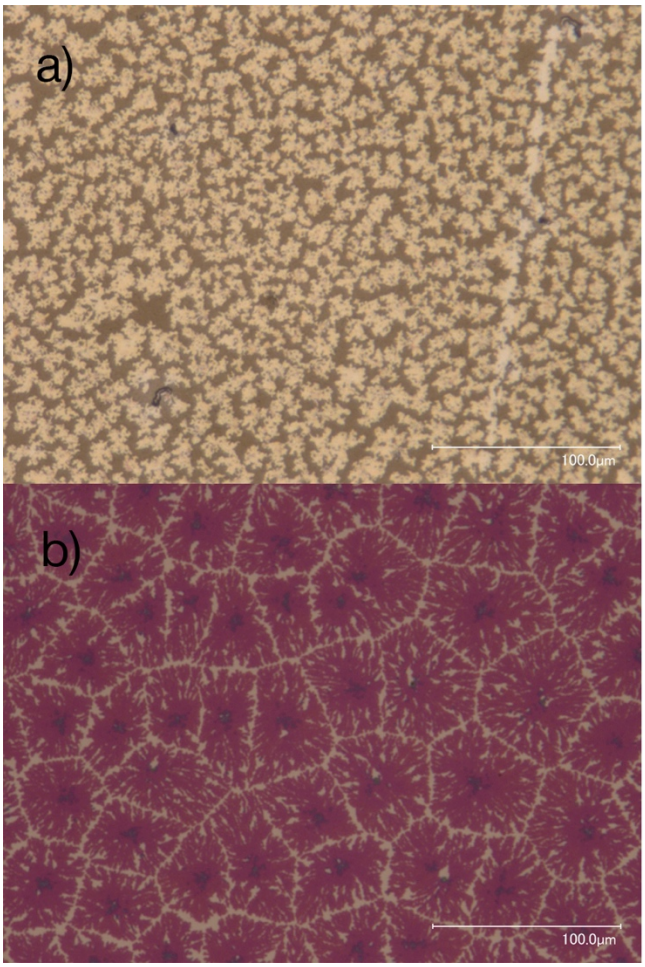

Figure. 3 (a) AIC on STO annealed at T_a=450 ℃ for 4 hours, in-situ image from top view (b) AIC on glass, Si grains and grain boundaries

Using Electron backscatter diffraction (EBSD) scanning, the orientation of AIC films grew under thin film regime and thick film regime were both characterized, and surprisingly showed (111) Si thin film growth. As shown in pole figures in Fig. 4, AIC thin film showed better quality of (111) Si growth with a more complete ring shape in (a), and AIC thick film gave a more random orientated Si crystallization in (c). In perspective of in plane orientation for AIC thin film, since the collected data in the pole figure showed a ring shape in Fig. 4 (a), instead of concentrated points, the Si grains were disorientated in-plane. In EBSD scan Fig. 4 (b), the images showed consistency of blue (111) Si growth in AIC thin film, and the red (100) area were from back (100) STO substrate. But in EBSD scan for AIC thick film on STO in Fig. 4 (d), Si grains were mostly randomly orientated. The results were surprising, because as shown in *Kurosawa et al.* AIC Si orientation map in Fig. 2, Si should have grown in (100) direction, because in the thin film regime Si atoms nucleate on Al/STO substrate, and since (100) Si and STO are lattice matched, (100) Si should be obtained. But pole figure of EBSD showed (111) preferential-crystal orientated Si grew on STO in t_{Al} < 50nm regime.

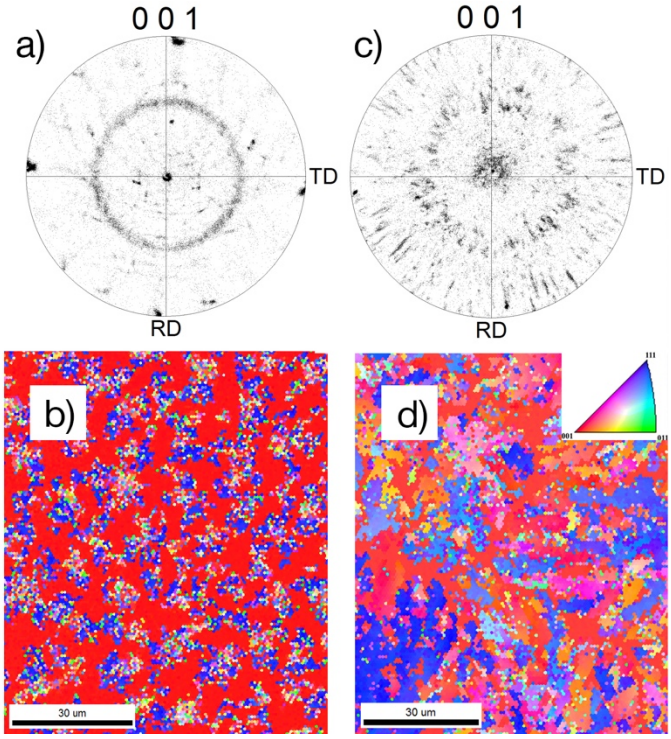

Fig. 4 (a) & (b) EBSD scan for AIC thin film on STO (c) & (d) EBSD scan for AIC thick film on STO

Such behavior was further proved in XRD scan that (111) Si film on STO was prepared in the thin film regime. In Fig. 5 (a), an intensity peak was detected at 27 degree, which corresponded to (111) Si signal, but no (100) Si peak was detected. In Fig. 5 (b), in the same thin film regime, Si grew in (100) direction on (100) Si substrate, and not (111) signal was detected. Hence, in homoepitaxial growth, (111) Si could not be grown. But when AIC was performed on hetero-substrate, (111) orientated Si was preferential instead of (100).

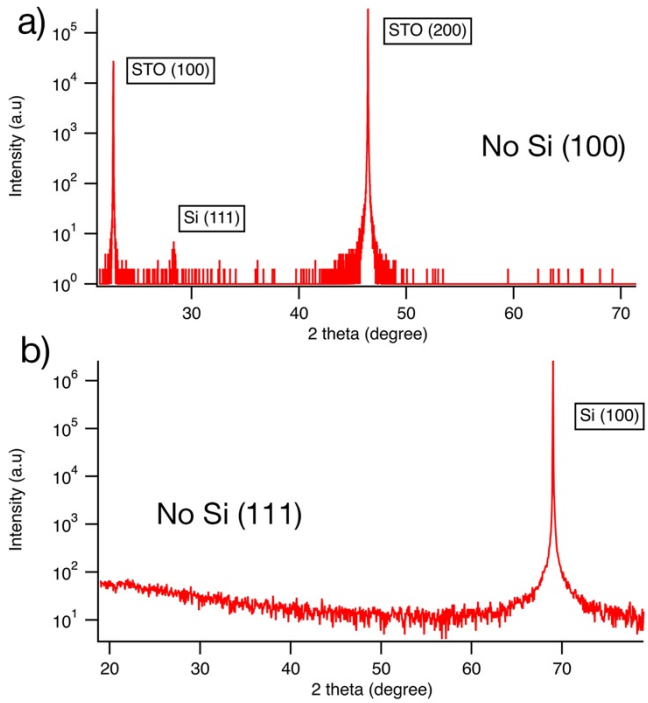

Fig. 5 XRD scan for (a) AIC thin film on STO (b) AIC thin film on Si (100)

The same results were observed in AIC Si on glass experiment as AIC Si on STO, shown in Fig. 6. In the thin film regime, (111) preferential-crystal Si film was found to grow on glass, but in thicker regime, random orientated Si film was observed. Since the glass substrate was amorphous, lattice match has no influence on Si growth. When Si atoms reached Al/glass interface, they nucleated at the lowest interfacial energy level in the (111) direction. Hence the (111) Si preferentially grew on glass substrate. The similar results of AIC Si on glass and AIC Si on STO showed that substrate has minimal effect on Si crystallization, so that (111) Si may be grown on other different substrates in the thin film regime.

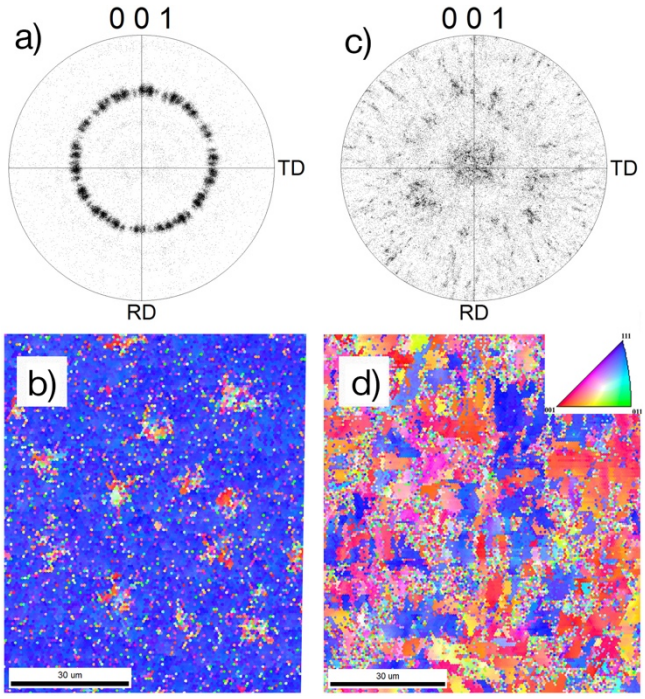

Fig. 6 (a) & (b) EBSD scan for AIC thin film on glass (c) & (d) EBSD scan for AIC thick film on glass triangle

In the future, more AIC Si on STO samples would be done to grow larger and more coalescence (111) Si grains. TEM characterization would be done on current samples to analyze how the (111) Si grew on (100) STO without an epitaxial relation. AIC would be researched on other crystalline substrates that are lattice mismatch with (111) Si, for the further study of how AIC Si grown on other different substrates.

ACKNOWLEDGEMENTS

The author wishes to thank Dr. Mel F. Hainey Jr. for guidance through the project. The author would like to thank Professor. Noritaka Usami and Professor. Kazuhiro Gotoh for providing the laboratory environment. The author would also thank lab members of Usami laboratory for teaching the use of equipment. The author acknowledges the support from JUACEP program and JSPS research fellowship.

REFERENCES

[1] M. Kurosawa, et al. Solid-State Electronics, 60(1), 7–12, (2011). http://doi.org/10.1016/j.sse.2011.01.033
[2] M. Kawasaki, et al. Science 266, 5190 (1994). doi: 10.1126/science.266.5190.1540
[3] M. Kurosawa, et al. Journal of Applied Physics 116, 173510 (2014). doi: 10.1063/1.4901262

[4] M. F. Hainey Jr., et al. Journal of Applied Physics 121, 115301 (2017). doi: 10.1063/1.4978706

INVESTIGATING THE MECHANICAL PROPERTIES OF CNT SHEET FILMS

P. Verberne

Mechanics and Aerospace Design Laboratory
Department of Mechanical and Industrial Engineering, University of Toronto
verberne@mie.utoronto.ca

Supervisor: Prof. Y. Ju

Material Characterization and Mechanics Laboratory
Department of Micro-Nano Mechanical Science and Engineering, Nagoya University
ju@mech.nagoya-u.ac.jp

ABSTRACT

Optimal conditions for dry-spinning CNT sheets was employed to develop conductive, translucent, flexible PET – CNT films. The electrical, optical, thermal and electromechanical behaviours of these films were investigated. It was found that the films had a mean resistance of 1100±300 Ω and optical transmissivity of 90.5%. The films is capable of low power heat generation with a temperature increase of $80°C$ at a supplied power of 3.5 W. The applied voltage can be reduced by increasing the resistivity of the film allowing for tailoring for the desired application. The electromechanical response under tensile loading determined that conductivity is maintained up to 100% strain. Additionally, there is a highly nonlinear relation between the resistivity and the applied strain which can indicate failure of the film.

1. INTRODUCTION

Carbon nanotubes have excellent chemical, thermal, mechanical and electrical properties [1-3]. Consequentially, there is significant interest in using this material for numerous applications to take advantage of these properties. One of the methods to utilize carbon nanotubes is through CNT films. These films can either be thought of as CNTs embedded within a polymeric matrix or CNTs deposited on a polymeric substrate. Due to their unique properties CNT films have numerous potential applications. This is because of their unique and outstanding properties such as high transparency, conductivity and flexibility that are relatively uniform over the entire film [1, 4]. Owing to the stretchability of the films they can be used within biological and medical applications e.g., prosthetic limbs, artificial skin, artificial muscle, medical devices or soft robotics [4, 5]. Numerous sensors could be developed using these films to measure pressure or strain, measure the pH of solutions, or the ability to detect the presence of harmful gases and potentially remove them [4, 6-8]. Finally there are numerous electronic applications, flexible conducting displays, super capacitors and solar cells [2-4, 9-11].

There are various methods to create CNT thin films, but can be classified by the fabrication environment, solid, liquid or gas phase. For solid-phase fabrication, CNTs are grown on a rigid substrate and are then detached from and transferred to the flexible substrate. They are predominantly produced through three methods, arc – discharge, laser ablation, and chemical vapour deposition (CVD) [12-14]. CVD is the most common method and can be used to create randomly distributed or aligned CNTs films. The CNTs are then either transferred to the film or they are drawn from the synthesized array to create the highly aligned films [13, 14]. The advantage solid-phase fabrication is that the process can be a single step and does not require pre-synthesized material. Unfortunately, quantity, reliability and reproducibility of these sheets are a current limitation [14,15]. For liquid phase fabrication, CNTs are dispersed through sonication in a volatile solvent that rapidly evaporates. This solution can be transferred to the flexible substrate through various methods including spin-coating, inkjet printing, draw-down rod coating and nanoimprinting [12-14, 16, 17]. These methods for film creation are reliably reproducible in laboratory environments and can be scaled up for commercial applications. However, there are numerous steps associated with the production and the harsh chemicals have a negative effect on the electrical properties of the film [12, 14]. To overcome some of the disadvantages of liquid phase fabrication, gas phase fabrication was developed. Using

atmospheric-pressure floating-catalyst chemical vapour deposition CNTs are continuously grown. Immediately after synthesis, these CNTs are directly deposited onto the flexible substrate at room temperature [13, 18, 19].

Even though there have been successful implementation of CNT films for these applications challenges remain. One of the predominate challenges is the scalability of the current manufacturing techniques for mass production and to increase the size of films reliably [1, 3, 5]. Other challenges are related to the transference of the material properties to the film, reliable production of the CNT sheets, improvements to the physical and material properties of the films, and improving the sensitivity, stability and durability of the films [1, 3, 5]. Therefore, this report will investigate some of these issues by developing conductive, translucent, flexible PET – CNT films, with dry-spun CNT sheets drawn from optimal grown CNT arrays. The electrical, optical, thermal and electromechanical characteristics of these films are investigated.

2. EXPERIMENTAL METHOD

The MWCNT arrays were fabricated by thermal chemical vapour deposition (CVD) using iron film as the catalyst. The CNTs were grown on a silicon substrate that was coated with a 200 nm layer of SiO_2, 3 nm layer of Al_2O_3 and final the iron film. These layers were deposited through electron beam evaporation and the thickness was monitored by using a quartz-crystal sensor. The CNT growth occurred in a CVD chamber consisting of a quartz tube with a diameter of 46 mm. At either end of the tube there were stainless steel ends allowing for the inflow and outflow of the gases. The heater was placed at the centre of the tube. The chamber was evacuated of air and filled with a mixture of Ar, C_2H_4 and H_2 gas and the flow of the mixture was constant at 520 sscm, with the Ar gas at 400 sscm and the combined mixture of C_2H_4 and H_2 at 120 sscm.

Since the reliable spinnability of the CNT forest was paramount to create CNT arrays, the parameters associated with the CNT array growth were previously investigated. Through previous work conducted it was determined that the optimal conditions for are at a temperature of 750 °C, Fe thickness between 1.0 – 2.0 nm, and gas flow ratio between 70:50 to 100:20 (C_2H_4 : H_2) sccm. These conditions ensured that the CNT array synthesized had reliable and repeatable spinnability allowing for the creation of the CNT arrays in this work. The ramping rate for the heat was $40°C/\text{min}$.

As shown in Fig. 1 (a) these method produced a high density CNT array with a CNT length of 240 µm. From this

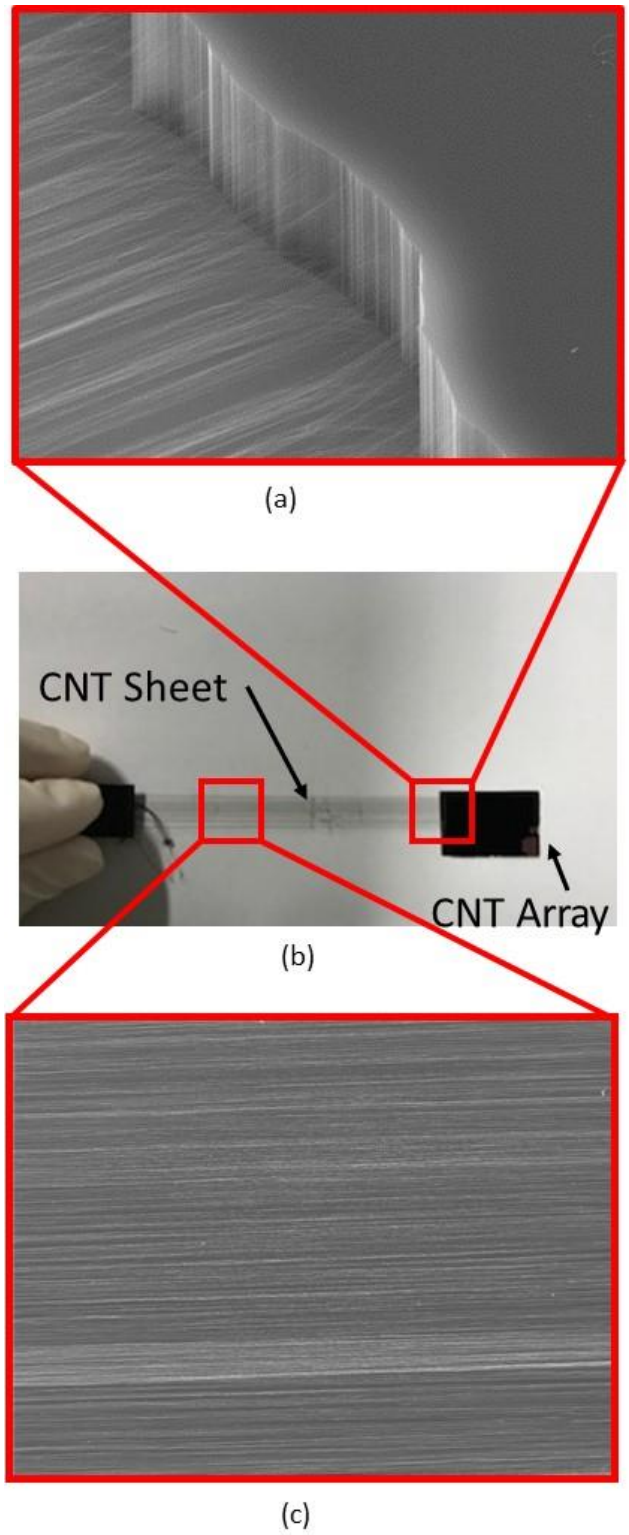

Fig. 1: The produced CNT array and CNT sheet; (a) the SEM micrograph of the CNT array produced using CVD under optimal conditions (b) the drawing out process used to create the CNT sheet, and (c) the SEM micrograph for the CNT sheet showing the highly aligned CNT.

array it was possible to draw out the CNT array using the simple method of adhesive tape to initiate the drawing process, with the subsequent CNTs latching together due to van der Waal forces. This allowed arrays of up to 200 mm in length to be drawn out as shown in Fig. 1 (b). To create the flexible CNT film, PET was used as the substrate material with dimensions of 100 x 60 x 0.125 mm for the CNT arrays to be deposited on. THE PET film was cut to the desired dimensions and cleaned with ethanol to remove any containments and to increase the adhesion of the CNT to the PET film. The CNT array was drawn out repeatedly and deposited on the PET film until the entire film was covered with the CNT arrays. This proved to be a simple and effective method to create the flexible translucent CNT films. Once the PET was covered a thin layer of silver paste was applied on either perpendicular to the CNT sheet orientation to connect all of the sheets to form a connective film. The film with the silver paste was cured at room temperature in a partial vacuum overnight.

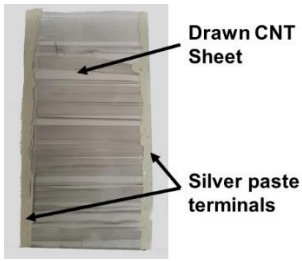

Fig. 2: Developed PET – CNT sheet film

3. RESULTS AND DISCUSSION

3.1 FILM PROPERTIES

First, the electrical properties of the films were established to determine the resistivity of the produced samples. This was measured through an Agilent U1242B multimeter. It was found that the PET – CNT films have a resistivity of 1100±300 Ω. This shows that the produced samples are conductive in nature and are capable of being used in a circuit. Additionally, it indicated that the films can be tailored to have varying resistances to allow for customization in certain applications. Further work is necessary to reduce the variability of the produced samples and to determine the parameters/ values dictating the resistivity.

Another important factor is the transparency of the film after applying the CNT sheets to it. To give a preliminary indication of the transparency of the CNT film the light transmission was measured through a light sensor from a mobile device [20]. The light intensity was measured several times for each film and was averaged over the entire film to provide the average light intensity transmitted through the film. The equation that can quantify the transmittance is as follows,

$$T = \frac{I}{I_0} \times 100$$

where T is transmittance percentage, I is detected light intensity, I_0 is initial light intensity. Due to the fact that the PET film supporting the CNTs does not transmit all of the light through the material, we cannot use the intensity of the light source but rather we must compare to the intensity of the light transmitted through the PET film. Through this method it was first determined that the PET film has a transparency of $87.1 \pm 1.0\%$. When the CNTs are applied relative to the light intensity from the PET film, the transmittance is $90.5 \pm 1.6\%$. This clearly indicates that the CNT sheet has high transparency which is reinforced through Fig. 3.

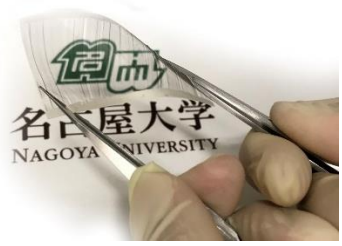

Fig. 3: Demonstration of the transparency and flexibility of developed film

3.2 USE IN ELECTRICAL CIRCUIT

Due to the conductive nature of the PET – CNT film first a simple demonstration of the capabilities was conducted by implementing it in a simple circuit. The circuit consisted of a constant voltage source, the film and a light bulb. Part of the circuit is shown in Fig. 4. When comparing the circuit before and after the inclusion of the film, it was found that the power necessary to emit light was significantly higher than without the film. During observations significant heat was being produced from the film.

Fig. 4: Demonstration of the conductive ability of the PET – CNT film.

3.3 LOW-POWER RESISTIVE HEATER

While examining the electrical circuit in the preceding section it was observed that the CNT sheet film resistor was dissipating a significant amount of energy through the heating of the film as indicated by the melting of the film. Therefore, a thorough examination of the thermal generation properties of the film was undertaken. To conduct this aspect of the work the CNT film was directly connected to a variable DC power supply. For this experiment Texio PSF-400L was used for this purpose. Wires were attached on either end of the CNT film as shown in Fig. 5. A constant current was supplied in increments of 10 mA to the CNT film and the voltage was measured from the aforementioned multimeter. The resulting temperature of the CNT film was measured through a Fluke 568 Infrared Thermometer. This allowed for the examination of the temperature variation over the CNT film to examine any localized heating.

Through this experiment it was possible to determine the thermal response of the film. Fig. 6 shows the nonlinear relationship of the maximum temperature increase for an applied voltage. Additionally, it is shown that for higher film resistivity the same temperature increase can be achieved through a lower voltage. However, the 900 Ω film seems to be an anomaly due to its erratic response. This is confirmed in Fig. 7 when the maximum temperature increase is compared to the applied power. There is a linear relationship between the applied power and temperature increase as expected. However, for the 900 Ω film it deviates from the other samples.

While measuring the maximum temperature increase, it was observed that the temperature was not constant over the entirety of the film. It was found that the maximum temperature usually occurred further away from the connections to the power supply, i.e., at the top of the film in Fig. 5. This was confirmed by swapping the orientation of the film and observing that the maximum temperature once again occurred at the furthest point away from the power supply connection. Currently, it is unknown why this is occurring and further work is needed.

Finally, while obtaining the results, it was found that eventually the applied power was too high and it resulted in localized melting of the film as shown in Fig. 8. From Fig. 7 this corresponded to an applied power of 3.5 W. The interesting aspect of this melting is that it did not directly occur at the locations of maximum temperature previously discussed. This indicates that the localized melting could be occurring due to the creation of very high temperatures due

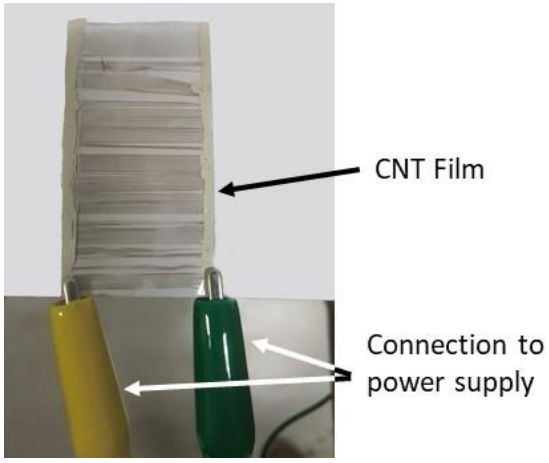

Fig. 5: Experimental setup for conducting the thermal heating of the CNT film.

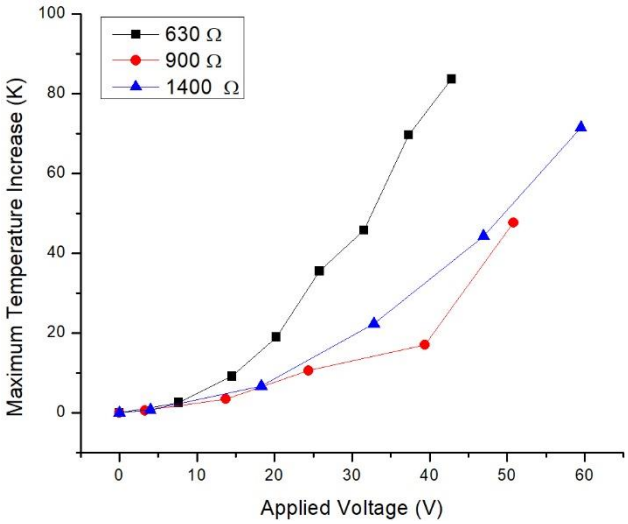

Fig. 6: Effect of film resistance on the maximum temperature increase for applied voltage

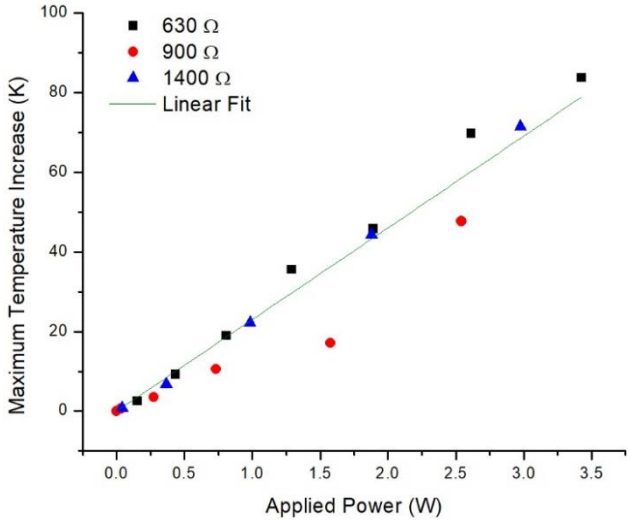

Fig. 7: Comparison of the maximum temperature increase with respect to applied power.

to higher resistances at these localized areas. This could indicate that there are defects in the CNT sheet resulting in the splicing of the CNT strand resulting in a small gap. This gap would not conduct until the applied power is high enough either cause a dielectric breakdown of the plastic or electrical arcing between the two ends of the strands. Further examination of this phenomena must be undertaken to determine the underlying cause.

3.4 ELECTROMECHANICAL RESPONSE

Tensile testing of the films was conducted to determine the electromechanical response and determine the suitability of these films for structural health monitoring. Tensile testing was conducted with a Shimadzu AGS-X 5 kN tester under constant velocity at a rate of 2 mm/min. To allow for the samples to be secured in the grips it was necessary to reduce their dimensions. The previously produced samples were cut to a dimension of 25 x 60 mm, as a consequence this increased the initial resistance of samples. The samples were placed within the grips with rubber spacers surrounding the samples to reduce the possibility of conductivity through the grips and ensure that the grips do not damage the delicate film under loading. Wires were attached to the silver paste and connected to the aforementioned multimeter to measure the electrical response under loading. An overview of the experimental set up is shown in Fig. 9.

The change in the resistivity of the samples compared to the elongation of the sample is shown in Fig. 10. The resistance of the samples was normalized with respect to the initial resistance of the sample to account for the varying initial resistance between samples. As shown in the graph, the response of the films resistivity is nonlinear. For low deformations the change in the resistivity is very minor. Therefore, a strain amplifier must be used to quantify these changes. However, for very large strains the change is very pronounced due to the highly nonlinear behaviour. For the samples examined conductivity is maintained up to 100% strain. Please note that Sample 3 was slipping in the grip beyond 80% and therefore never reached the maximum loading condition.

Additionally, for Sample 1 there are two distinct regions were there are near vertical increases in the resistances; see Fig. 10. These regions correspond to the failure of the film while under loading. The first increase was at 100% strain where a small section of the film failed, as shown in Fig. 11 (a) through the failure of the top left portion. The second rapid increase was at 130% strain and this corresponded to the

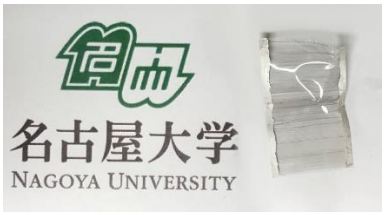

Fig. 8: Localized melting of the film.

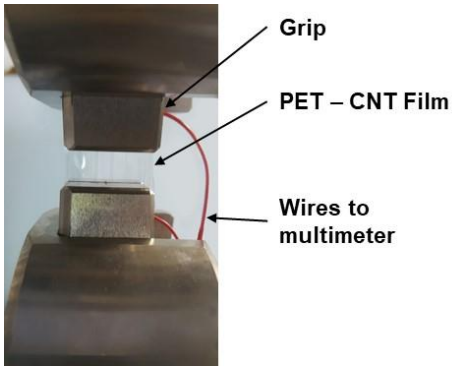

Fig. 9: Tensile testing of PET – CNT film.

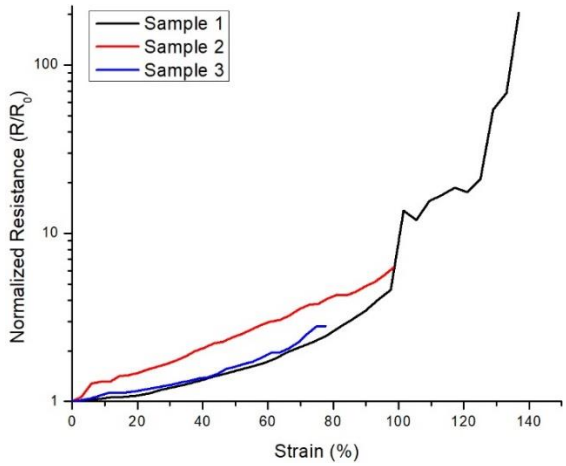

Fig. 10: Normalized resistivity response of the film under tensile loading

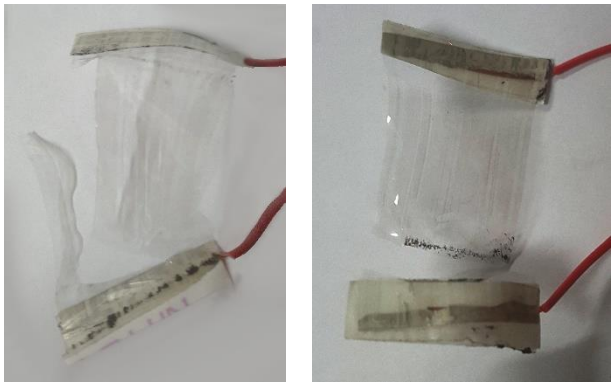

(a) **(b)**

Fig. 11: Comparison of film failure for (a) Sample 1, and (b) Sample 2.

bottom section tearing under load, as indicated in Fig. 11(a). The rate of increase was less than the first localized failure since there was a progression of the failure surface. Eventually, the resistivity of the film exceeded the measurement capabilities of the multimeter. In contrast, the failure of Sample 2 did not undergo this repeated process. The failure of this sample was very sudden as the entire bottom surface of the sample failed nearly instantaneously, as shown in Fig. 11 (b). Due to the rapid progression of the failure there was no prior indication through the resistivity of the film that the failure would occur.

4. CONCLUSIONS

This work examined the electrical, optical, thermal and electromechanical behaviours of flexible PET – CNT films. The creation of these films utilized CNT sheets drawn from CNT arrays through dry-spinning. These arrays were synthesized under optimal conditions to ensure the reliability and repeatability of these arrays. The produced films are flexible and translucent allowing for optical transmissivity of 90.5%. The films are capable of low power heat generation with a temperature increase of $80°C$ at a supplied power of 3.5 W. The increased resistance of the films reduces the applied voltage necessary. However, it has been observed that the temperature distribution is not constant over the film, and there is the potential of localized melting of the film through an unknown process. Finally, the electromechanical response under tensile loading determined that conductivity is maintained up to 100% strain. Additionally, there is a highly nonlinear relation between the resistivity and the applied strain which can indicate failure of the film.

ACKNOWLEDGEMENTS

This work was supported by the Material Characterization and Mechanics Laboratory led by Professor Ju of Nagoya University. In particular, I would like to extend my sincere gratitude to Professor Ju for accepting me to conduct this research through JUACEP. Additionally, I would like to acknowledge the guidance provided by Taguchi Takuto for the completion of this project.

REFERENCES

[1] Du, J., Pei, S., Ma, L., & Cheng, H. M. 25th anniversary article: carbon nanotube-and graphene-based transparent conductive films for optoelectronic devices. *Advanced materials*, 26(13), 1958-1991, (2014).

[2] Lv, T., Liu, M., Zhu, D., Gan, L., & Chen, T. (2018). Nanocarbon-Based Materials for Flexible All-Solid-State Supercapacitors. *Advanced Materials*, *30*(17), 1705489.

[3] Jung, D., Han, M. E., & Lee, G. S. (2014). pH-sensing characteristics of multi-walled carbon nanotube sheet. *Materials Letters*, *116*, 57-60.

[4] Park, S., Vosguerichian, M., & Bao, Z. A review of fabrication and applications of carbon nanotube film-based flexible electronics. *Nanoscale*, *5*(5), 1727-1752, (2013).

[5] Trung, T. Q., & Lee, N. E. Materials and devices for transparent stretchable electronics. *Journal of Materials Chemistry C*, 5(9), 2202-2222, (2017).

[6] Jung, D., Han, M., & Lee, G. S. Room-temperature gas sensor using carbon nanotube with cobalt oxides. *Sensors and Actuators B: Chemical*, *204*, 596-601, (2014).

[7] Yildiz, O., & Bradford, P. D. Aligned carbon nanotube sheet high efficiency particulate air filters. *Carbon*, *64*, 295-304, (2013).

[8] Keyi, Y. A. N., Toku, Y., Morita, Y., & Ju, Y. (2018). Fabrication of multiwall carbon nanotube sheet based hydrogen sensor on a stacking multi-layer structure. *Nanotechnology*.

[9] Lipomi, D. J., & Bao, Z. Stretchable, elastic materials and devices for solar energy conversion. *Energy & Environmental Science*, *4*(9), 3314-3328, (2011).

[10] Ulbricht, R., et al. Transparent carbon nanotube sheets as 3-D charge collectors in organic solar cells. *Solar Energy Materials and Solar Cells*, *91*(5), 416-419, (2007).

[11] De Volder, M. F., Tawfick, S. H., Baughman, R. H., & Hart, A. J. Carbon nanotubes: present and future commercial applications. *science*, *339*(6119), 535-539, (2013).

[12] Sun, D. M., Liu, C., Ren, W. C., & Cheng, H. M. A Review of Carbon Nanotube-and Graphene-Based Flexible Thin-Film Transistors. *Small*, *9*(8), 1188-1205, (2013).

[13] Hu, L., Hecht, D. S., & Gruner, G. Carbon nanotube thin films: fabrication, properties, and applications. *Chemical reviews*, *110*(10), 5790-5844, (2010).

[14] Janas, D., & Koziol, K. K. A review of production methods of carbon nanotube and graphene thin films for electrothermal applications. *Nanoscale*, *6*(6), 3037-3045, (2014).

[15] Wang, C., Zhang, J., Ryu, K., Badmaev, A., De Arco, L. G., & Zhou, C. Wafer-scale fabrication of separated carbon nanotube thin-film transistors for display applications. *Nano Letters*, *9*(12), 4285-4291, (2009).

[16] Song, J. et al. (2009). The production of transparent carbon nanotube field emitters using inkjet printing. *Physica E: Low-dimensional Systems and Nanostructures*, *41*(8), 1513-1516.

[17] Dan, B., Irvin, G. C., & Pasquali, M. (2009). Continuous and scalable fabrication of transparent conducting carbon nanotube films. *ACS nano*, *3*(4), 835-843.

[18] Zavodchikova, M. Y., et al. Carbon nanotube thin film transistors based on aerosol methods. *Nanotechnology*, *20*(8), 085201, (2009).

[19] Sun, D. M., et al. Flexible high-performance carbon nanotube integrated circuits. *Nature nanotechnology*, *6*(3), 156, (2011).

[20] Gutierrez-Martinez, J. M., Castillo-Martinez, A., Medina-Merodio, J. A., Aguado-Delgado, J., & Martinez-Herraiz, J. J. Smartphones as a Light Measurement Tool: Case of Study. *Applied Sciences*, *7*(6), 616, (2017).

(b) The 22nd JUACEP Workshop

for the summer research course students from University of Michigan, UCLA and University of Toronto

Date: Monday, August 27, 2018
Venue: NIC Conference Room (3rd floor, NIC)

[Timetable]

10:00 – 10:05	Opening address Prof. Norimi Mizutani, Dean of Graduate School of Engineering
10:05 – 10:20	**(1) Petrus Verberne**, *Adviser: Prof. Y. Ju, Micro-Nano Mechanical Science and Engineering* "Investigating of Mechanical Properties of Functionalized CNT Sheet Films" ***(P.40)***
10:20 – 10:35	**(2) Chenhui Zhou**, Adviser: Prof. N. Usami, Materials Process Engineering "Aluminum Induced Crystallization on STO Substrate" ***(P.43)***
10:35 – 10:50	**(3) Fadi Rafeedi,** *Adviser: Prof. Y. Hasegawa, Micro-Nano Mechanical Science and Engineering* "Controlling Flower Stick Rotation Using 3D Vision Feedback" ***(Undisclosed)***
10:50 – 11:05	**(4) Sida Li**, *Adviser: Assoc. Prof. K. Niitsu, Electrical Engineering* "Gate Leakage Based Timer Design for Biomedical Devices" ***(Undisclosed)***
11:05 – 11:15	Break
11:15 – 11:30	**(5) Ziming Song**, *Adviser: Assoc. Prof. T. Miwa, Civil Engineering* "Optimizing Rural Bus Network in Toyota City" ***(P.45)***
11:30 – 11:45	**(6) Xuan Yang**, *Adviser: Prof. Y. Yamada, Mechanical Systems Engineering* "Evaluation of Gait Stability in the Use of a Wearable Walking Assist Device" ***(P.48)***
11:45 – 12:00	**(7) Guanqun Yang**, *Adviser: Prof. Y. Yamada, Mechanical Systems Engineering* "Autonomous Motion Planning of a Mobile Robot by Use of Deep Reinforcement Leaning for Fall Prevention in Hospital" ***(P.50)***
12:00 – 12:10	Completion ceremony
12:30 –	Farewell banquet at Chez Ziroud

**10 minutes presentation + 4 minutes Q&A each*

Investigating the mechanical properties of functionalized CNT sheet films

Pieter Verberne

Mechanics and Aerospace Design Laboratory
University of Toronto

Supervisor: Professor Y. Ju

Material Characterization and Mechanics Laboratory
Nagoya University

August 27th, 2018

1

Presentation Outline

- Introduction
- Objectives
- Experimental Method
- Results
- Conclusion
- Future Work

2

Introduction

- Carbon nanotubes (CNTs) have unique material properties.
  - **Young's Modulus** ~ 1 TPa
  - **Aspect Ratio** ~ 1000's
  - **Tensile Strength** ~ 100 GPa
  - **Electrical Conductivity** ~ 2 x 10^6 S/m
  - **Thermal Conductivity** ~ 6000 W/mK

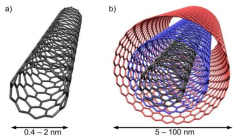

Single-walled (SWCNT) **Multi-walled (MWCNT)**

- The length of CNTs is usually only around several micrometers.
- Drawn CNT sheets can increase the effective length

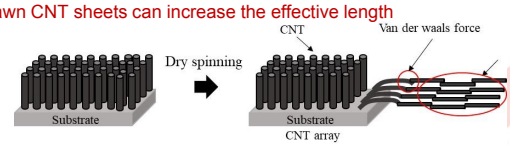

Schematic of CNT sheet formation

3

Statement of Problem

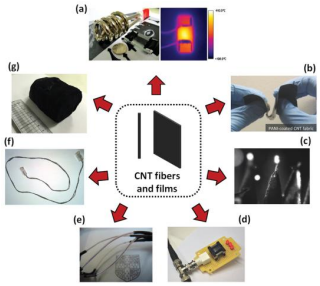

Applications for CNT films and fibers [1]

- CNT sheets can be used as films and have great potential to improve current and future applications.
- However, CNT films have challenges associated with:
  - High quality synthesis
  - Scalability
  - Transference of properties
  - Usability in applications

4

Objectives

1. Learn, observe and apply the current synthesis techniques that produce high quality CNT arrays that can reliably and repeatedly produce CNT sheets through dry-spinning.
2. Utilize these sheets to create conductive, flexible, transparent CNT films that can be utilized for various applications.
3. Examine the optical, electrical, electromechanical and thermal response of CNT films and the potential applications.
4. Investigate functionalized CNT films to address some of the existing challenges and examine potential applications.

5

Experimental Method

6

Substrate Preparation

Film formation by electron beam vapor deposition

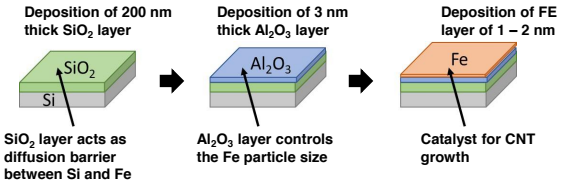

Table 1 Condition of EB vapor deposition for each material.

Material	Pressure [Pa]	Evaporation rate [nm/s]	Thickness [nm]
SiO_2	1.0×10^{-3}	0.2	200
Al_2O_3	6.0×10^{-4}	0.1	3
Fe	6.0×10^{-4}	0.1	1.0 – 2.0

7

CNT Sheet Growth

CNT synthesized through chemical vapor deposition

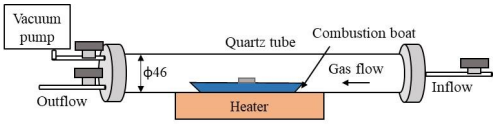

Schematic of CVD chamber for CNT growth

Table 2: Conditions for CVD

Property	Value	Property	Value
Heating rate [℃/min]	40	Ar gas flow [sccm]	400
Growth temperature [℃]	750	C_2H_4 gas flow [sccm]	70 - 100
Growth time [min]	15	H_2 gas flow [sccm]	20 - 50
		Total flow [sccm]	520

8

Dry Spinning of CNT Sheet

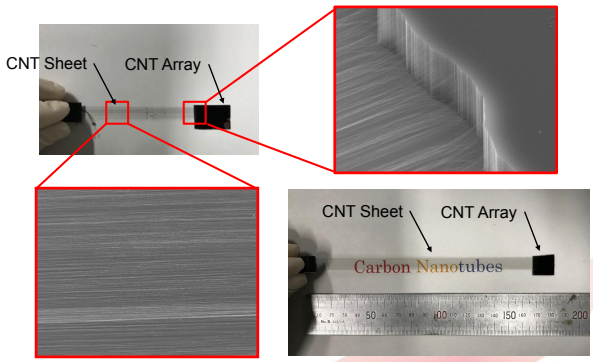

9

Development of PET – CNT Film

Procedure:

- The substrate for the film was a PET sheet with dimensions of 100 x 60 x 0.125 mm.
- First the PET film was wiped with an ethanol solution to remove contaminants and improve adhesion of CNT sheet.
- A single layer thick CNT sheet was repeatedly drawn out onto the PET film and cut at the edge.
- Once the PET was covered, silver paste was applied on either end and was cured in a partial vacuum overnight.

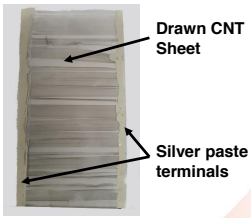

Developed PET – CNT sheet film

10

Results

11

PET – CNT Sheet Film Properties

Electrical Properties:

- A multimeter was used to determine the electrical properties
- The PET – CNT film has a resistivity of $1100 \pm 300\ \Omega$.

Optical Properties:

- A light sensor was used to determine the transparency of the film
- The transmittance of the PET – CNT film is $90.5 \pm 1.6\%$ compared to the bare PET film.

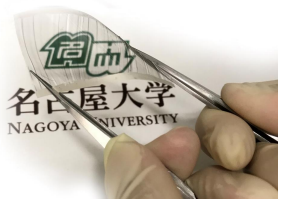

Demonstration of the transparency and flexibility of developed film

$$T = \frac{I}{I_0} \times 100\%$$

12

Electrical Response of Film

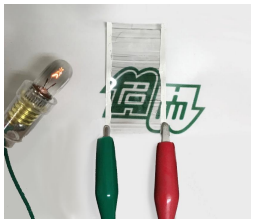

Demonstration of conductive ability of PET – CNT film

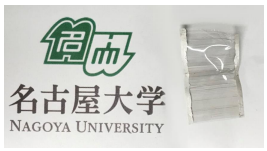

Localized melting of film

- The conductivity of the PET – CNT film is demonstrated by implementing it in a simple circuit.
- There was significant energy loss due to heat generation, which resulted in localized melting of the film.

13

Thermal Generation of Film

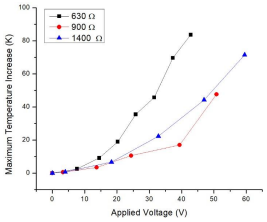

Maximum temperature increase for applied voltage

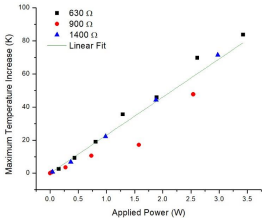

Maximum temperature increase by applied power

- The thermal behaviour was investigated by supplying a constant direct current to the film and measuring the temperature increase.
- The PET – CNT film has a linear relation to the applied power independent of resistivity.
- The maximum power that the film can currently withstand is ~3.5 W

14

Electromechanical Response of Film

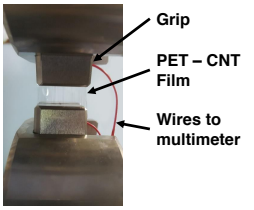

Tensile testing of PET – CNT film

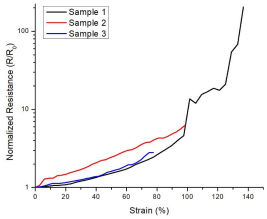

Maximum temperature increase by applied power

- Tensile testing of the films was conducted to determine the electromechanical response.
- The response of the films resistivity is nonlinear and the rapid jumps indicate failure.
- Conductivity is maintained up to 100% strain.

15

Conclusions

1. Successfully applied current methods for producing high quality, consistent, and repeatable CNT sheets through dry-spinning.
2. Implemented these sheets to create conductive, flexible, transparent PET – CNT films.
3. Determined that the optical transmittance of the PET – CNT film is 90.5±1.6%.
4. Examined the thermal response for the films and determine the linear response of the temperature increase to the applied power.
5. Investigated the nonlinear electromechanical response of the films under mechanical loading and determined that conductivity is maintained up to 100% strain.

16

Future Work

- Investigate a method of developing functionalized CNT films accounting for current challenges.
- Compare the results of the functionalized CNT films to the results presented in this work to contrast the difference.
- Utilize the functionalized CNT films for applications, such as, high sensitivity strain gauges, gas sensor, biomedical sensors.

17

References

1. Janas, D., & Koziol, K. K., Carbon nanotube fibers and films: synthesis, applications and perspectives of the direct-spinning method. *Nanoscale*, *8*(47), 19475-19490 (2016).

19

Aluminum Induced Crystallization of Si Thin Film on STO substrate

Chenhui Zhou
Usami Laboratory
8/27/18

UCLA

NAGOYA UNIVERSITY

Introduction

Aluminum-induced crystallization (AIC) is a method of growing high-quality continuous polycrystalline silicon (poly-Si) layers onto different substrates

(100) Si is the primary substrate in CMOS processing device

In this experiment, Si on STO was selected to research on solid state heteroepitaxial growth. (100) Si thin film was expected to grow on (100) $SrTiO_3$ substrate since (100) Si is lattice matched to the STO, but (111) Si film was grown on (100) $SrTiO_3$ substrate when AIC was performed within thin film regime (t_{Al} < 50 nm).

M. Kurosawa, et al. Journal of Applied Physics 116, 173510 (2014). doi: 10.1063/1.4901262

Layer exchange mechanism of AIC

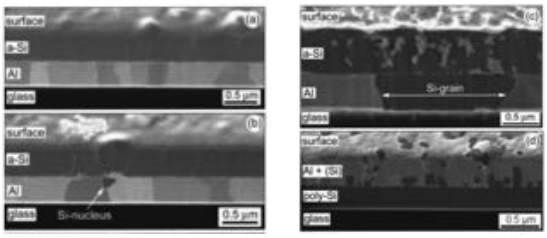

a-Si/Al/glass structure: (a) before annealing, (b) after annealing for 5 min, (c) 10 min, and (d) 60 min at 500 ° C

O. Nast, et al. Journal of Applied Physics 88, 124 (2000); doi: 10.1063/1.373632

Why d_{Al}<50nm thin film regime?

Group B: (>50 nm regime): Si nucleates at Al/Al-oxide interface, forming (100) orientated Si, 80% (100) was produced

Group C: (< 50 nm regime): Si nucleates at Al/Substrate interface, forming (111) orientated Si, 95% (111) was produced

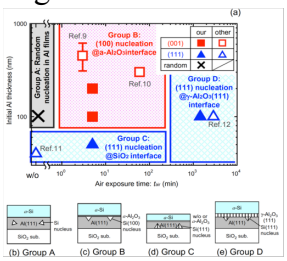

AIC Si orientation map, air exposure time t_{air} and initial Al thickness t_{Al} dependent
(b)-(e) model for preferential Si nucleation for Group A-D

M. Kurosawa et al. / Solid-State Electronics 60 (2011) 7–12

Why on STO?

Si has diamond crystal structure, STO has perovskite structure

(100) Si was expected to grow on (100) STO due to lattice match

The surface unit cell of (100) Si is rotated 45° , the lattice constant of a 1*1 surface cell is 3.84 Å, which is very close to 3.905 Å of cubic STO

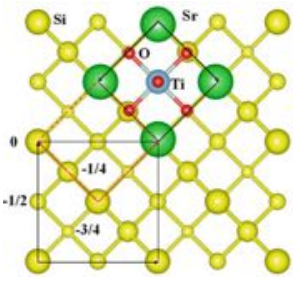

Epitaxial matching of STO and Si (001)

Growth Method

Structure: a-Si/Al-oxide/Al/STO
Cleaning: Buffered NH_4F-HF (pH = 4.5) pretreatment 10 min
IPA/di water 10 min sonification
RF Sputtering: 110W power
1.1 A/s Al and 0.8 A/s a-Si
Structure: a-Si/Al-oxide/Al/STO
Annealing: 450 °C 4hr/ 500 °C 2hr in 0.5 sccm Ar
Etching: 5% HF 20 seconds to etch away top Al layer

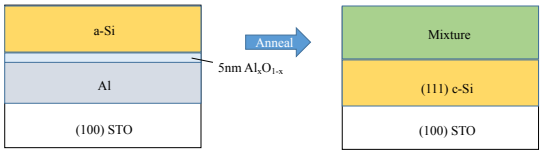

Grain growth

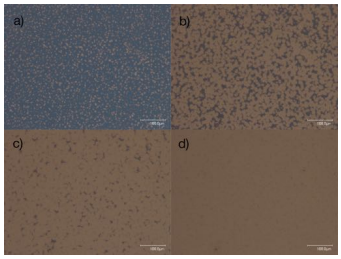

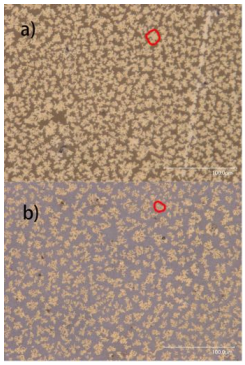

(a)-(d) Al and Si layers exchange at 450 ℃ (a) at 2 min (b) 6min (c) 12 min (d) 15 min

M. Kurosawa, et al. Journal of Applied Physics 116, 173510 (2014). doi: 10.1063/1.4901262

Characterization

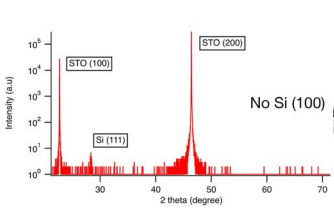

XRD scan for AIC thin film on STO

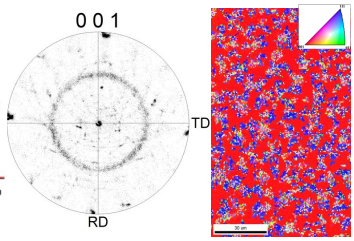

EBSD scan for AIC thin film on STO

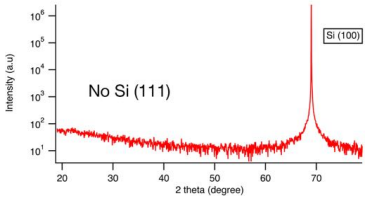

XRD scan for AIC thin film on Si (100)

In homoepitaxial growth, (111) Si can not be grown

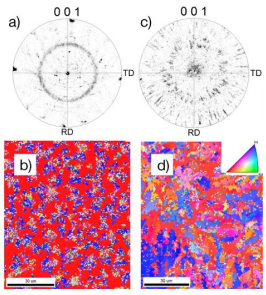

(a) & (b) EBSD scan for AIC thin film on STO (c) & (d) EBSD scan for AIC thick film on STO

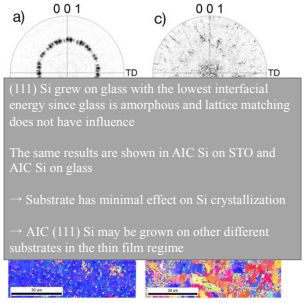

(111) Si grew on glass with the lowest interfacial energy since glass is amorphous and lattice matching does not have influence

The same results are shown in AIC Si on STO and AIC Si on glass

→ Substrate has minimal effect on Si crystallization

→ AIC (111) Si may be grown on other different substrates in the thin film regime

(a) & (b) EBSD scan for AIC thin film on glass (c) & (d) EBSD scan for AIC thick film on glass

Future Work

- AIC films on STO in thin film regime to optimize the size and coalescence of (111) Si grains
- TEM characterization on current samples to analyze how (111) Si grow on (100) STO
- Other crystalline substrates may be used for further study of how AIC Si grown on different substrates

Acknowledgement

➢Prof. Usami, Prof. Gotoh, Prof. Kurosawa, Dr. Hainey Jr.
➢Lab members
➢JUACEP program and Kato san

Optimization of Rural Bus Network in Toyota City

Ziming Song
Supervisor: Prof. Tomio Miwa

Outline

- Introduction
- Optimization Algorithm
- Solution Formulation
- Objective Selection
- Proposed Solution
- Conclusion
- Question and Answer Session

Introduction

- Toyota City is the second most populous city in Aichi Prefecture
- Consists city part and rural part
- Rural Part has Aging Population
- Aging Population needs to use bus service to go shopping and doctor visits
- Current set up involves a branch route and key routes
- A transfer from branch route to key routes is required
- Optimization on Current Route Network is needed

Introduction

Figure 1- Toyota City Bus Network[1]

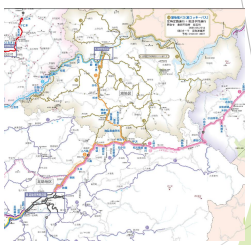

Figure 2- Asahi Region Bus Network[1]

Optimization Algorithm

- Linear Program
  - Mathematical Program that has a linear objective function with linear constraints
  - Standard Form:
    - $Maximize\ C^T x$
    - $subject\ to\ Ax \leq b$
      $0 \leq x$
- Transportation Problem Model
  - Special case of a linear program
  - Focusing on Transporting people/goods from one location to another
  - Focus on minimize the cost while meet the constraints.
  - Sample Transportation Network:

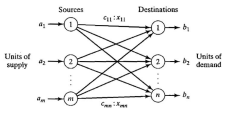

Figure 3- Sample Transportation Network[2]

Optimization Algorithm

- Traveling Salesman Problem [2] [3]
  - Goal: Shortest Travel Distance
  - Can be modified
  - Standard Formulation:
  - $x_{ij} = \begin{cases} 1, if\ city\ j\ is\ reached\ from\ city\ i \\ 0, otherwise \end{cases}$
  - $Minimize\ z = \sum_{i=1}^{n}\sum_{j=1}^{n} d_{ij}x_{ij}, d_{ij} = \infty\ for\ all\ i\ and\ j$
  - Subject to:
    - $\sum_{j=1}^{n} x_{ij} = 1,\ i = 1,2,\dots,n$
    - $\sum_{i=1}^{n} x_{ij} = 1,\ i = 1,2,\dots,n$
    - $x_{ij} = (0,1)$
- Heuristics [2]
  - Focus on getting good solution instead of Optimum Solution
  - Simulated Annealing
  - Genetics Algorithm
  - Takes time to compute

Solution Formulation

- The bus route optimization problem can be formulated as a traveling salesman problem
- Use the same objective function as traveling salesman problem
- Modify the constraint such the must visit places in Asuke is included in all trips.
- Combine the Key lines and branch lines into one line.
- Different day and time will have a different route and schedule

7

Objective Selection

- Bus route optimization is a multi objective optimization problem
- Multi objective optimization problem does not usually produce the optimum solution
- Simplify the multi objective optimization problem can reduce the complexity
- The two most important objectives:
  - Operating Cost- Minimize
  - Service Coverage- Maximize

8

Objective Selection

- Equations for the Cost is below:
  - $C_{True} = C_{Total} - R_{Tickets}$
  - $C_{Total} = C_{Fuel} + C_{Driver} + C_{Other}$
  - $R_{Tickets} = N_{passenger} * D * 25$

9

Objective Selection

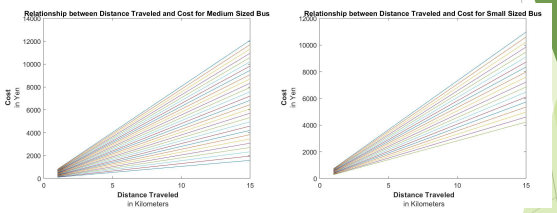

10

Objective Selection

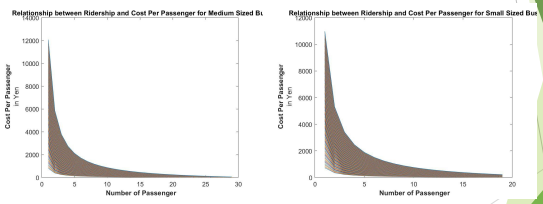

11

Proposed Solution

- Current Bus Network
- 1 Key Route
- 2 Branch Routes
- Raw Cost per round trip: 39000 yen

- Optimized Bus Network:
- 2 Combined routes
- Raw Cost per round trip 30000 yen
- Cost Saving: 22.2%

12

Conclusion

- Optimized bus service saves operating cost for Toyota city
- Optimized bus service also saves cost for local residents
- Optimized bus service saves the travel time for local residents
- Only the preliminary results is obtained during the program due to time constraint
- In the future, more algorithms can be developed for this optimization problem
- In the future, more programs can be developed to solve this optimization problem

13

Reference

[1] Toyota City, "Digital Map: Toyota City Bus Map", 2018. [Online]. Available: http://michinavitoyota.jp/portal/pdf/bus/busmap_b_201804.pdf

[2] H.Taha, Operations Research. Upper Saddle River, NJ: Prentice Hall, 2007

[3] J.Yu, "Traveling Salesman Problems", [Online]. Available: https://optimization.mccormick.northwestern.edu/index.php/Traveling_salesman_problems

14

Acknowledgement

- Special thanks to Miwa Sensei for letting me have this research opportunity and support during the whole duration of this research based program
- Special thanks to TA Jiang Feng and Huang Xinyi for helping me to get familiarized with the Nagoya University and NUTREND lab.
- Special thanks to Kato San and other staff for their work to make this program happen.

15

EVALUATION OF GAIT STABILITY IN THE USE OF A WEARABLE WALKING ASSIST DEVICE

Presenter: Xuan Yang
Supervisor: Prof. Yoji Yamada
Lab: Yamada Lab

Overview

- Introduction and Previous Work
- XCoM Concept & Key Parameters
- Definition of Local Coordinate
- Results & Discussions
- Summary

Introduction

Wearable Walking-Assist Robot

- Help with gait rehabilitation
- Decrease the risk of tripping
- Improve life quality of the elderly
- Could be used in daily life

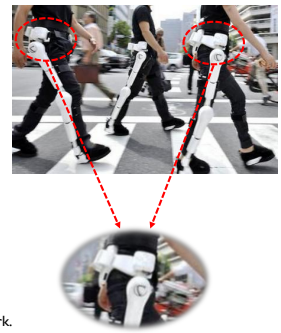

Limitation & Challenge

- Lose degree of freedom at hip joint
- Cannot curve easily

My Work

- Analyze gait stability based on previous work.
- Compare gait stability in restricted and unrestricted hip joint condition during curving.

Curving Experiment using Walking-Assist Device

Walking-assist Device

- Degree of freedom at hip joint could be restricted or released.

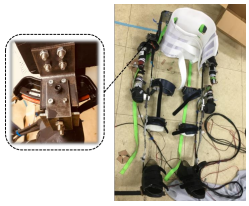

Experiments

- 40 trials by a male subject.
- 20 trials in restricted condition.
- 20 trials in unrestricted condition.

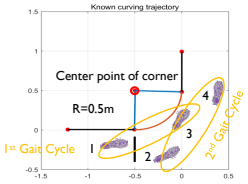

Data

- Follow a known curving trajectory.
- Data of 4 steps were recorded and mainly focus on the 2nd cycle.
- Separate first step using left foot from the one using right foot.
- Data recorded every 0.01s.

[1] Fukui Y, Akiyama Y, Yamada Y, et al. The change of gait motion when curving a corner owing to the motion restriction caused by a wearable device[C]//Systems, Man, and Cybernetics (SMC), 2017 IEEE International Conference on. IEEE, 2017: 525-530.

XCoM Concept & Key Parameters

1. Extrapolated **CoM**: $\mathbf{XCoM} = \mathbf{CoM} + \frac{\mathbf{V}_{CoM}}{\omega_0}$

2. Eigen-frequency: $\omega_0 = \sqrt{\frac{g}{l}}$

l: Pendulum length defined as maximum height of CoM in each trial and mean value of all trials. (Restricted and unrestricted conditions are calculated separately.)

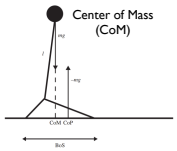

Fig.1 Inverted pendulum human model

3. Base of Support (BoS):
   - Relative to ground reaction force.
   - Based on location of foot.

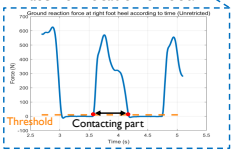

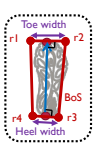

BoS with one foot on ground

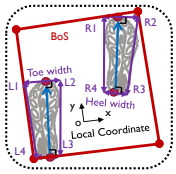

BoS with both feet on ground

[2] Bruijn S M, Meijer O G, Beek P J, et al. Assessing the stability of human locomotion: a review of current measures[J]. Journal of the Royal Society Interface, 2013, 10(83): 20120999.

Key Parameters & Definition of Local Coordinate

4. Margin of stability: $\mathbf{b} = \mathbf{BoS} - \mathbf{XCoM}$

In y direction (Forward position):

$$b_y = (max)BoS_y - XCoM_y$$

In x direction (Lateral direction):

$$b_x = \begin{cases} XCoM_x - (min)BoS_x & V_{CoM_x} < 0 \\ (max)BoS_x - XCoM_x & V_{CoM_x} > 0 \end{cases}$$

- XCoM is always near maximum BoS in y direction.
- b could be largely affected by V_{CoM} in x direction.
- Smaller b means less stable.

❖ **Definition of Local Coordinate**

X unit vector: $\vec{X} = \frac{\vec{P}_{R.ASIS} - \vec{P}_{L.ASIS}}{\left\|\vec{P}_{R.ASIS} - \vec{P}_{L.ASIS}\right\|} = (X_x, X_y)$

Y unit vector: $\vec{Y} = \begin{bmatrix} 0 & -1 \\ 1 & 0 \end{bmatrix} \vec{X} = (Y_x, Y_y)$

(Rotating X axis 90° to the left is Y axis.)

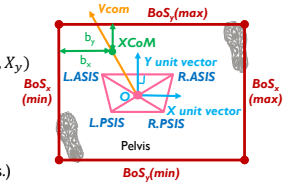

$(X_x, X_y), (Y_x, Y_y)$ is coordinates of Y unit vector expressed in global coordinates.

Results & Discussions

1. Forward Stability

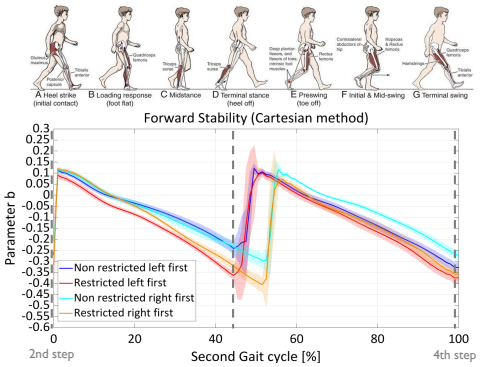

https://www.google.co.jp/search?q=walking+gait+cycle&rlz=1C1CHZL_zhCNUS765US765&tbm=isch&tbo=u&source=univ&sa=X&ved=2ahUKEwjCjPCv0IjdAhUPdc4KHbevAvoQsAR6BAgFEAE&biw=1536&bih=709#imgrc=X-Ny-Xfd-l-hmM:

Results & Discussions

2. Lateral Stability

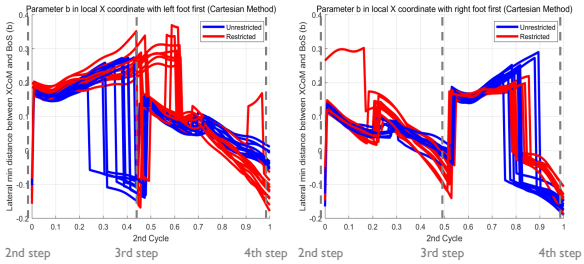

- The most unstable situation happens just before the heel contact at each step.
- Lateral gait stability needs to be further analyzed.

Results & Discussions

3. Further Analysis on Lateral Stability

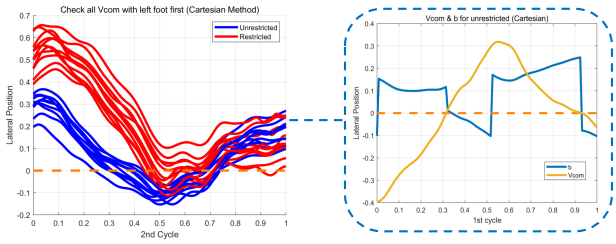

- b jumps when velocity of CoM changes sign.
- The time to change velocity direction is not consistent.
- Cases b do not jump only happen in restricted condition.
- Non-jumping cases are omitted.

Results & Discussions

4. Margin of gait stability at each step

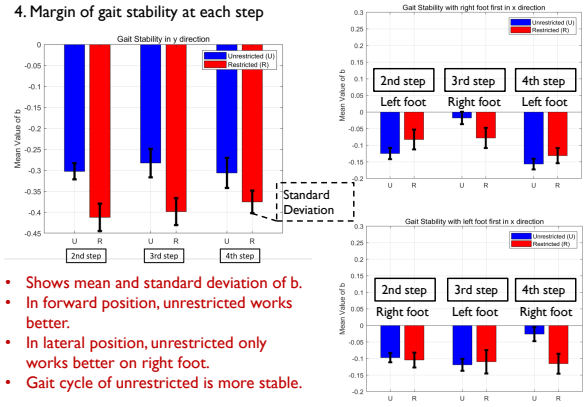

- Shows mean and standard deviation of b.
- In forward position, unrestricted works better.
- In lateral position, unrestricted only works better on right foot.
- Gait cycle of unrestricted is more stable.

Summary

Work done:

- Performed XCoM concept to analyse gait stability.
- Estimated margin of stability on unrestricted and restricted condition.
- Compared gait stability on both conditions based on margin of stability.

Effects in restricted condition:

- Less stable in forward position.
- Negative influence on in time direction changing.
- Perturb gait cycle.
- More stable on inner foot during curving in lateral position.
- Less stable on outer foot in lateral position.

A Study on Autonomous Motion Planning of Mobile Robot by Use of Deep Reinforcement Learning for Fall Prevention in Hospital

Guanqun Yang

University of California, Los Angeles
Department of Electrical and Computer Engineering

Japan-US-Canada Advanced Collaborative Education Program, 2018

UCLA

Outline

UCLA

Background

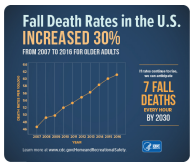

- Number of elderly-involved accidents is growing.
  - Most are related to unexpected falls.
- Elderly care service becomes unaffordable.
  - Average elderly care service could cost more than $6844 per month (as of 2016).

1. Suitable for repetitive duties
2. Higher efficiency and accuracy

Insight

Mobile robot could take a role in elderly care service, specially fall prevention.

UCLA

Background

- Number of elderly-involved accidents is growing.
  - Most are related to unexpected falls.
- Elderly care service becomes unaffordable.
  - Average elderly care service could cost more than $6844 per month (as of 2016).

1. Suitable for repetitive duties
2. Higher efficiency and accuracy

Insight

Mobile robot could take a role in elderly care service, specially fall prevention.

UCLA

Objective

- Detect a safe route
- Lead the user to his/her destination

Result: Secure Path
Input: Environment Map
while *map not fully explored* **do**
  exploring environment and detecting dangers;
  if *danger detected* **then**
    DangerLevel = DangerEvaluation();
    DangerSpotAnnotation(DangerLevel);
  else
    SafetySpotAnnotation();
  end
end
SecurePath = MotionPlanning();

- Involving indoor mapping, object detection and path planning.
- Individually accomplished by DL, SLAM and RL.

UCLA

Hospital Scene Dataset Preparation

- The requisite of applying object detection network to our application.
- No application-specific dataset is available.
- Create dataset from scratch.

Table: Statistics of Dataset

Number of Categories	Number of Images	Image Size
29	2900	256×256

UCLA

Object Detection Based on YOLO

Detection Framework	mAP	FPS
Fast R-CNN	70.0	0.5
Faster R-CNN ResNet	76.4	5
Faster R-CNN VGG-16	73.2	7
SSD300	74.3	46
SSD500	76.8	19
YOLO 256 × 256	69.0	91

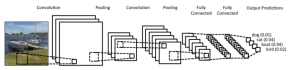

- A real-time detection system with high accuracy
- Fine tune the network to suit our purpose

Network Fine-tuning Procedure

1. Size and similarity of customized dataset
2. Large dataset: fine tuning entire network regardless of similarity
   Small dataset: only allowed when similarity is low

Experimental Result

- Fine-tuned object detection system could detect items previously not applicable.
- Real time detection in video stream

Experimental Result

- Fine-tuned object detection system could detect items previously not applicable.
- Real time detection in video stream

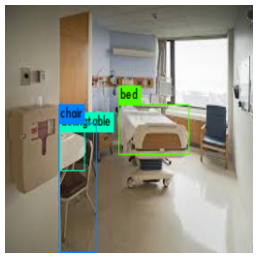

Reinforcement Learning-Based Motion Planning

- Trial and error learning through interaction to achieve optimal action sequence

Start	-1	0
0	-1	0
0	0	10

Problem State

- Markov Decision Process ($\langle S, A, P, R, s_0 \rangle$)
  1. $s_t \in S$, s_0 and $a_t \in A$: state, initial state and action
  2. $P(s_{t+1}|s_t, a_t)$: system dynamics
  3. $R(s_{t+1}|s_t, a_t)$: reward

- Could be solved with dynamic programming (DP)

Result: Optimal action $\pi(s)$ at each state s
for $k = 1 : \infty$ **do**
  $V_k[s] = \max_a \sum_{s'} P(s'|s,a)R(s\prime|s,a) + \gamma V_{k-1}[s']$;
  if $\forall s$, $|V_k(s) - V_{k-1}(s)| < \epsilon$ **then**
    $\pi(s) = \text{argmax}_a \sum_{s'} P(s'|s,a)R(s\prime|s,a) + \gamma V_{k-1}[s']$;
  end
end

Experimental Result

- Providing an annotated map
  - Complicated danger distribution
- One secure route could be autonomously detected.

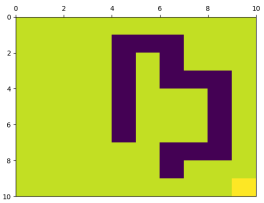

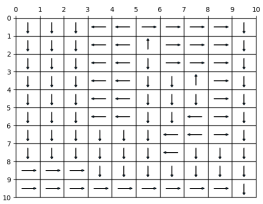

Summary

What Has Been Done

- A hospital scene-specific dataset
- Application of YOLO in hospital scene
- Previously environment from expert ⇒ Autonomous and precise perception of environment

Future Work

- Collecting more data for dataset
- Integration of entire system

<3> Classes and Events

(a) JUACEP Summer Program 2018　Japanese Course Syllabus

Course name	Japanese Language
Teaching staff	Ms. YASUI Sumie　(TA…　Sinpeng Songglod & Saito Yuri)
Course period	June 21 - July 26, 2018
Weekly timetable	Tuesday & Thursday, 3rd (45 min) & 4th period (90 min) (13:45-16:15)
Classroom	IB 101 Lecture room, 10th floor of IB North Building
Textbook	"GENKI An Integrated Course in Elementary Japanese" I　(The Japan Times) This textbook is a comprehensive approach to developing the four basic language skills (listening, speaking, reading and writing) in order to cultivate overall Japanese-language ability. *Some teaching material will be given in class.
Course Contents	**Course outline** The purpose of this course is to introduce the most essential Japanese words and expressions for everyday life. Students will learn writing system (Hiragana & Katakana), the basic grammar, expressions of Japanese. **Classroom activities** Basic communication skills required in everyday life will be taught by introducing new vocabulary, new grammar, and practicing listening, conversation and role-playings. **Homework and Quiz** You are expected to submit your homework by the deadline. Quizzes will be given every day in class. 1. Hiragana　2. Katakana 3. Dictation　4. Conjugation
Evaluation	1. Homework　20%　S=100-90 2. Quizzes　30%　A=89-80 3. Oral exam.　50%　B=79-70 100%　C=69-60 More than 80% attendance is required.　F(fail)=59-0 You will be officially awarded 1 credit of Nagoya University.

Course schedule	1. 6/21(Thu) Greeting Expressions, Hiragana 1 Introducing yourself , Noun sentences 1, Occupation, Nationality, Age, Numbers 1-100 2. 6/26(Tue) Classroom expressions, Hiragana 2 Shopping, Noun sentences 2, Price, Numbers 101-1,000,000 3. 6/28(Thu) Hiragana 3 Describing where things are, Locations Placing an order at a restaurant 4. 7/3(Tue) Hiragana 4 Talking about your daily life Verbal sentences 1, Time reference, Adverbs 5. 7/5(Thu) Hiragana 5 Invitations, Suggestions, Desires Verbal sentences 2, Days/Weeks/Months/Years, Counting 6. 7/10(Tue) Katakana 1 Talking about your family Adjectives, Likes or Dislikes, Degree expressions, Family terms 7. 7/17(Tue) Katakana 2 Talking about your week-end, Past tense, Time words 8. 7/19(Thu) Katakana 3 Making a request (Verb-Te-form), Progressive actions, Describing your status 9. 7/24(Tue) Asking permission, Prohibition, Negative request Describing two things Talking about your interests Plain form 10. 7/26(Thu) The Final Examination (speaking)

(b) Hands-on Exercise

"Disassembly and Assembly of Internal Combustion Engine"

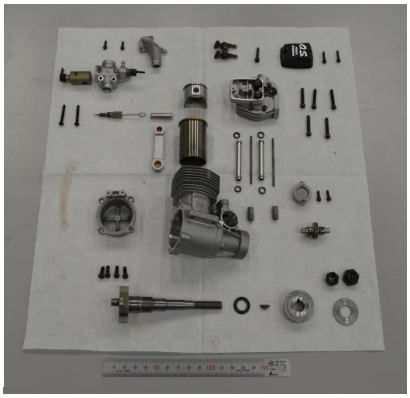

Date: 13:00 – 16:00, Monday 9 July 2018

Place: Creation Plaza, 10th floor of IB-North

Staff: Prof. Tsuyoshi Inoue, Director of Creation Plaza

Technical staff… Nakakimura, Goto, Saito, Isogai, Adachi and Yamamoto

Teaching Assistant…Feng, Kobayashi, Li, Fukui, Kim, Kamibeppu, Taguchi, Kuboki

Contents:

1. Opening remarks
2. Introduction to the basis of the Internal Combustion Engine and other engines
   (History, Characteristics, Operation principle, Demonstration of engines)
3. Disassembling → Assembling → Adjustment
4. Performance test
5. Jet engine demonstration
6. Discussion, questionnaire

(c) JUACEP Seminars

The 45th JUACEP Seminar

第 45 回 名古屋大学日米協働教育プログラムセミナー

13:30- Thursday, July 12, 2018
Lecture room 221 (2F, Eng.Bldg. II)

Droplet Microfluidic Tools for High-Throughput Single-Cell Assays

Prof. Katsuo Kurabayashi

Department of Mechanical Engineering
Department of Electrical Engineering
and Computer Science
University of Michigan, U.S.A.

Biography

Katsuo Kurabayashi is Professor of Mechanical Engineering and Electrical Engineering and Computer Science at the University of Michigan, Ann Arbor. He received his BS in Precision Engineering from the University of Tokyo in 1992, and his MS and PhD in Materials Science and Engineering from Stanford University, CA, in 1994 and 1998, respectively. His current research focuses on optofluidics, nanoplasmonic and biomolecular biosensing, and BioMEMS/microsystems for immunology, clinical diagnosis, and analytical chemistry. He received the 2001 NSF Early Faculty Career Development (CAREER) Award, and the Robert Caddell Memorial Award in 2005, the Pi Tau Sigma Outstanding Professor Award in 2007, the Mechanical Engineering Outstanding Achievement Award in 2013 from the University of Michigan, and the Ted Kennedy Family Team Excellence Award in 2015 from the College of Engineering at the University of Michigan.

Inquiry: JUACEP Office 日米協働教育プログラム (Ext. 2799)

JUACEP: Japan-US Advanced Collaborative Education Program, Graduate School of Engineering

The 46th JUACEP Seminar

第 46 回 名古屋大学日米協働教育プログラムセミナー

平成 30 年 7 月 13 日（金）10:30～

221 講義室（工学部２号館２階）

研究立案プロセスと論文の書き方

倉林活夫　教授 *JUACEP Coordinator*
Department of Mechanical Engineering and Electrical Engineering & Computer Science, University of Michigan

概要：研究立案には、問題の明確化、アプローチの選定、研究のインパクトの予想等のプロセスが必要となります。研究者としての成功は、研究発表の場や論文執筆の際に、いかに論理的に話の筋道を立てて情報を発信できるかにかかっています。このセミナーでは、そもそも工学系大学院教育においてなぜ研究活動が必要なのか、研究の基本的なプロセスをいかに身に着けるか、いかにインパクトのある研究論文を英文で書くことができるかということについて話を進めていきます。また、同時にミシガン大学工学部機械工学科の短い紹介も行います。

（講演言語：日本語）

略歴：1992年東京大学工学部精密工学科卒。1994年スタンフォード大学材料科学部修士号、1998年同大学Ph.D.取得。その後スタンフォード大学研究員を経て、2000年1月よりミシガン大学。現在の研究テーマは、生体・医療・環境分野の先端計測 マイクロ・ナノデバイス開発と基礎研究。これらの研究分野で5つの米国特許取得と80 本以上の論文・著書執筆。2001年 NSF Early Faculty Career Development Award、2005年 Robert Caddell Memorial Award for significant joint graduate student/faculty research contributions from the University of Michigan、2007年 Pi Tau Sigma Outstanding Professor Award、2013年 the University of Michigan ME Outstanding Achievement Award など多数授賞。

Inquiry: JUACEP Office 日米協働教育プログラム (Ext. 2799)

JUACEP: Japan-US Advanced Collaborative Education Program, Graduate School of Engineering

(d) Meet-up for JUACEP Students

(e) Field Trip

Date: July 27, Friday

Fee: 2,000 yen

Visiting spots:

・Toyota Kaikan Museum
http://www.toyota.co.jp/en/about_toyota/facility/toyota_kaikan/museum/

・Toyota Motor Plant Tours, Motomachi Plant
http://www.toyota.co.jp/en/about_toyota/facility/toyota_kaikan/index.html

・Asahi Brewery Nagoya
https://www.asahibeer.co.jp/brewery/language/english/#Nagoya

・Tokugawa Museum
http://www.tokugawa-art-museum.jp/en/

・Dinner (Chinese restaurant)

Attendant: Assist. Prof. Naoki Azuma and Tomoko Kato

Schedule:

Time	Event	Transportation
9:00	Meeting at Toyoda Auditorium	
9:10	Departure from Nagoya University	Hired bus
10:00	Toyota Kaikan Museum	
10:30	Toyota Plant Tour –Motomachi Plant	Toyota tour bus
13:00	Leaving Toyota and Lunch in the bus	Hired bus
13:40	Asahi Brewery Nagoya Tour	
15:00	Leaving Asahi Brewery	Hired bus
15:30	Tokugawa Museum	
17:00	Leaving Tokugawa Museum	Hired bus
18:00	Dinner	
19:30	Adjournment	

*Schedule above is tentative and may be changed.
*Wear sports shoes for safety of the factory tour.
*Photo is not allowed in the plant.

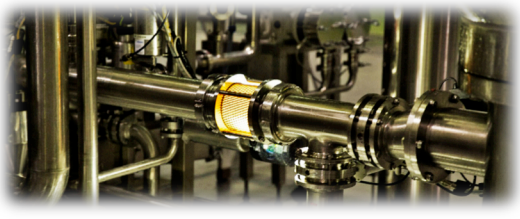

<3> Feedback and Questionnaires

Findings through JUACEP

Name: Sida Li
Affiliation at home country: Electrical Engineering at UCLA
Participated program: Summer Course 2018
Research theme: Gate Leakage Based Timer Design for Biomedical Devices
Advisor at Nagoya Univ: Prof Kiichi Niitsu
Affiliation at Nagoya Univ.: Electrical Engineering

The Japan US Advanced Collaborative Education Program has been one of the most meaningful and fulfilling summers. JUACEP not only offers a rare opportunity for engineering graduate students to experience studying abroad but also to advance their research and handling skills. During the program of the summer I was able to analyze, design, and perform, research on the design of oscillator for biomedical devices. This work is directly related to my own research at UCLA and it could be used to strengthen my PhD topic in my future work. Along with the immensely helpful knowledge and experience that came from my work within the framework of the summer program. I am working with my lab at Nagoya University to submit my results to a conference for publication.

the activities that the JUACEP office arranged are all very meaningful and interesting. For example, the field trip to Toyota factory introduced us the great history and future of the automotive industry. The Asahi factory showed us how to produce bottles of beer and provided us with unlimited drinking. The engine workshop provided us a great hand-on experience.

Outside the scheduled JUACEP activities, I was also able travel around Japan and see many places I wanted to visit. Moreover, Japan is closed to China. My girlfriend came to visit me during holiday and we have visited many places we have dreamed of going to in Japan.

Too many things happened in the 10 weeks that I cannot write down them all in one page. So here I just want say thanks to Nagoya University and JUACEP program for providing me with this precious opportunity to enjoy researching and exploring Japan.

Findings through JUACEP

Name:
Affiliation at home country (Dept & Univ):
UCLA Mechanical and Aerospace Engineering
Participated program: Summer Course 2018

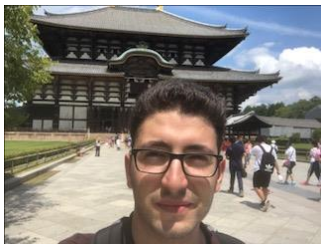

Research theme:
Advisor at Nagoya Univ: Prof. Hasegawa
Affiliation at Nagoya Univ. (Dept.): Micro-Nano Engineering

This summer was a very special one over all. Not only I was able to participate in research that is very interesting but also got to learn and experience the Japanese culture closely. I think this experience has improved my skills in robotics and gave a new perspective into other project that my colleagues were working on.

My research involved vision control of a nongrasping robot which juggles a devil stick. I have worked to fix an already existing robot and build a new environment for it. My work was very interesting and always got the chance to participate in other project and learn about new ideas that are being developed in this specific lab. My host Professor was extremely helpful with his guidance and feedback especially during the weekly meetings. Other members in the lab were also extremely nice and always willing to help with any situation. Sometime communication is hard, but we were able to understand each other at the end.

Living in Nagoya was nice, even though it is not a touristic city, but this gave us the opportunity to experience life in Japan rather than just being tourists. Nagoya has many beautiful places to go to and the University is also be nice. I tried to visit as many locations in Japan as possible with the amount of time I had. It was a great experience to visit all the major touristic locations. Transportation was a little confusing because of the tremendous number of train lines, but it became easier throughout my stay.

Over all this was one of my best experiences over all. I learned a lot from doing research and also had a lot of fun through program's activities and through my own travels.

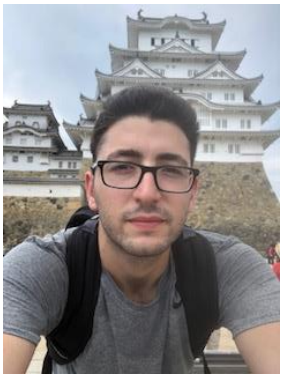

Findings through JUACEP

Name: Ziming Song
Affiliation at home country:
Industrial and Operations Engineering, Division of Integrative Systems and Design, University of Michigan
Participated program: Summer Course 2018

Research theme: Optimization of Rural Bus Network in Toyota City
Advisor at Nagoya Univ.: Associate Prof. Tomio Miwa
Affiliation at Nagoya Univ.: Department of Civil Engineering

Before I attend this program, I was always wondering about what is like to study and conducting in the Japan. As an international student study in the US experience the culture difference between my home country and US. Although I have visited Japan twice as a tourist before I attend this program but academic experience in another culture is a totally new experience to me. Fortunately, my supervisor Prof. Miwa is supportive if I have question regarding my research he is always available to answering me with in a quick time frame. Also, the TAs in my lab helped me to getting know the lab and equipment that I needed to do my research.

During my time in Japan I visited many new places that I've never been to in my previous trips to Japan. In the past I've visited most of the prefectures in Japan but I've never visited the Okinawa, Yamanashi, Kochi, Tokushima and Shimane prefectures. However in the weekends I took advantage and visited these places in different weekends.

In addition to the above, my experience in the Nagoya city is nice, Nagoya city has a fairly convenient public transportation network therefore I can visit different places in Nagoya easily. Also the living expense in Nagoya is very affordable compare to the living expense in the US. For example If I eat out for dinner in Ann Arbor I usually pay 15-20 US dollars for a meal in Asian restaurant. However in the Nagoya, I only need to pay 8-10 US dollars for a nice meal in the restaurants.

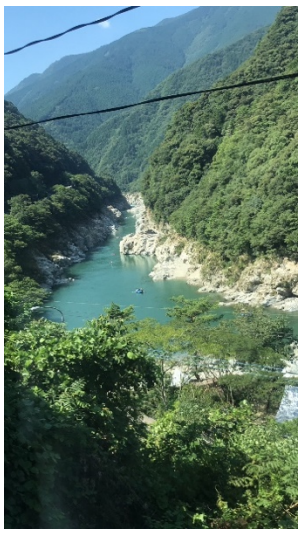

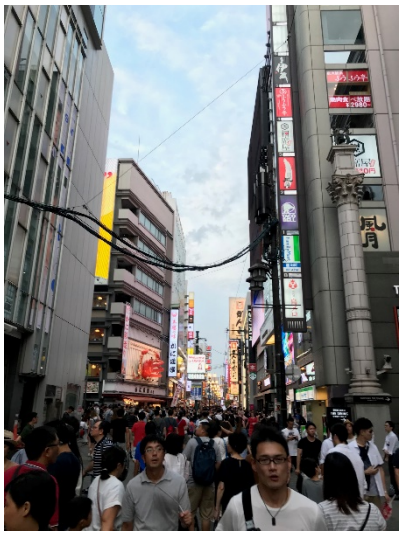

Findings through JUACEP

Name: Pieter Verberne
Affiliation at home country: Mechanical and Industrial Engineering, University of Toronto
Participated program: Summer Course 2018

Research theme: Investigating of mechanical properties of functionalized CNT sheet films
Advisor at Nagoya Univ: Professor Yang Ju
Affiliation at Nagoya Univ.: Department of Micro-Nano Mechanical Science and Engineering

When I was presented with the opportunity to go to Nagoya University to conduct research I was eager to attend. One of the primary reasons I was very interested in this exchange was to immerse myself in a different research environment and observe the difference in the research cultural between Japan and Canada. Additionally, through this program I was able to further expand my research interests and knowledge by conducting work that is extension to my primary thesis topic. Though I had some prior knowledge regarding this field, I never had enough time to dedicate to advancing my knowledge in the field. Through the program I greatly expanded my understanding of the principles of nanomechanics, methods for synthesizing CNT and CNT films, and the associated experimental techniques. This experience has given significant insights to this field and I believe this will greatly benefit my future career.

The predominant difficulty that I had during the exchange was my proficiency with the Japanese language. Coming to Japan I had no knowledge whatsoever regarding the language, coupled with the fact that learning languages is a difficulty of mine, I expected this to be a significant challenge. However, the Japanese class provided through the program greatly alleviated this difficulty. Though I am still very apprehensive speaking Japanese, I have been able to pick up on key phrases much better, increasing the positive interactions I have with others.

One of the greatest opportunities associated with this exchange is the ability to travel around Japan and experience the sights, culture and food. One of the first trips that I did while in Japan was going to Mount Fuji. Initially, I was only planning on climbing to the 7^{th} or 8^{th} station so that I was at least able to experience a portion of it. Owing to the progress that I was making I made the spur of the moment decision to climb all the way to the top. It was immensely rewarding, the views from the top were awe-inspiring and was a great personal achievement to climb all the way to the top. Furthermore, my parents were able to come visit me during the exchange and I was able to travel around with to Kiso Valley, Matsumoto, Takayama, Shirakawa-go, Kamikochi and Kyoto. This was the first time I travelled with my parents and it was a unique experience that I am especially grateful for that opportunity.

Overall, JUACEP was an amazing opportunity that I am eternal grateful for. I was able to make lifetime academic and personal connections and strengthen my own research abilities.

Findings through JUACEP

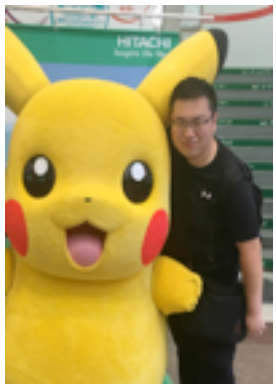

Name: Guanqun Yang
Affiliation at home country:
University of California, Los Angeles
Department of Electrical and Computer Engineering
Participated program: Summer Course 2018

Research theme: A Study of Autonomous Motion Planning of Mobile Robot By Use of Deep Reinforcement Learning for Fall Prevention In Hospital
Advisor at Nagoya Univ: Prof. Yoji Yamada
Affiliation at Nagoya Univ.: Department of Mechanical Engineering

The JUACEP is a program that enables us to collaborate with professors and students in Nagoya University to explore the field and topics of our interest. The experiences of this program will be discussed in three different aspects in the following.

The research atmosphere and academic community are different from both that of United States and China but many favorable features of these two are distilled into this institution, which is the leading research university in Japan. From the considerate mentorship and solid support of various hardware I need, I got into my research topic in a quite smooth fashion. Even though the heat is sometimes extreme here in summer, I find every single day pass very quickly since I got deeper into various fascinating algorithms and hardware that previously I had no access to.

The people and culture here also bear considerable difference from the countries I am familiar with, namely, China and United States. If one stay here for a relatively long period, he or she will not be amazed at the fact that so many quality products, something as small as a cable protector or something as large as cars, are designed or manufactured here. From my experience, the people here are so dedicated to their career and attempt to make every single detail all right. In fact, I truly like the deep learning platform -- Chainer since it resolves many configuration pains people will always encounter when they try to use TensorFlow and no wonder, it is created by a group of creative Japanese engineers.

One could anticipate disparate scenery when they come to Japan. Seemingly small in its territory, Japan, as the official slogan goes, have endless discoveries for you. During the JUACEP program, we have plenty of opportunities to visit different parts of Japan. We saw the prosperity and its preparation for 2020 in Tokyo. We felt the perseverance and optimism of this country when Kumamoto castle is reconstructed from every original brick and when local people are striving for normal life when ever-recorded rain hit Hiroshima. We also witnessed the broad horizon we have not seen for a long time in Hokkaido.

I would absolutely recommend this program to anyone who is interested in. Hopefully this program will continue to benefit more students.

Findings through JUACEP

Name: Xuan Yang
Affiliation at home country:
Mechanical and Aerospace Engineering, University of California, Los Angeles
Participated program: JUACEP Summer Course 2018

Research theme:
Evaluation of gait stability in the use of a walking-assist device
Advisor at Nagoya Univ: Prof. Yoji Yamada
Affiliation at Nagoya Univ.: Mechanical Engineering

This was my first time to go to Japan. I've always dreamed of traveling in Japan and experience Japanese culture once from my childhood. This program made my dream come true. Not only did it give me the opportunity to have a sightseeing trip where I want to go, but also served as a precious chance for me to study and learn new knowledge in Japan.

I got to know my great professor and sensei, make Japanese friends and learn more Japanese. My research here is to analyze the gait stability in the use of a wearable walking-assist robot. This was also my first time to see this kind of amazing and helpful robot, which could prevent people who have trouble in walking from falling or tripping. I still remember the first day I came to Nagoya University. I was so excited and couldn't wait to experience everything like snacks, buying something in a コンビニ, having a meal in 食堂 on campus, etc. That day I met my TA 久保木君 for the first time. He was so nice and friendly to me and showed me around campus for the whole afternoon, even though he still had a lot of part-time jobs to do. I could say that day served as a happy and exciting day for me as well as a bad luck day. I lost my first stipend due to my excessive rapture and carelessness, which was really a great loss. My joy and excitement completely vanished but the sense of shame and regret overwhelmed. I told my TA. He helped to search for it with me and told Ms Kato at the same time. I was so impressed and touched that I found nearly all the stuff on campus began to help me look for my stipend. Not up to half an hour, one of them found my stipend and gave it back to me. I was so appreciated and felt the warmth and kindness of Japanese people.

Luckily, there was another JUACEP student Guanqun Yang, also from UCLA, working in Yamada's lab, the same lab as mine. We worked in the same lab and our seats were near. Gradually, we became close friends and always travelled together during holidays. We went lots of places like Kumamoto, Hiroshima, Osaka, Tokyo, Kyoto, Nara, Kagoshima, etc. He loves lamen. So he led me tried many different types of lamen in Japan. My favorite is 中本蒙古らあ麺. Since we both love animations. Every time we went to a new place, we'd surely spend several hours hanging around animate store, though we still had trouble reading Japanese. We were even lucky enough to see World Cosplay Competition. I'd like to put some interesting and memorable photos here:




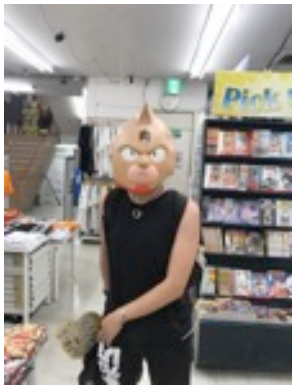

A Memorable Journey in Japan

Name: Chenhui Zhou
Affiliation at home country (Dept & Univ): UCLA
Participated program: Summer Course 2018

Research theme: Aluminum induced crystallization of Si on STO substrate
Advisor at Nagoya Univ: Prof. Noritaka Usami
Affiliation at Nagoya Univ. (Dept.): Materials Process Engineering

It has been a wonderful experience for me this summer. I worked as a graduate researcher with Dr. Mel F. Hainey Jr. in Professor Noritaka Usami laboratory. I spent a lot of time not only on doing research but also had fun with other lab members and got involved in the culture here. The laboratory members are very friendly, and when I had problems of using lab equipment, they taught me step to step patiently. Dr. Hainey Jr. kindly guided me through the whole project and made sure I had understood the project and results. I also had chances to play basketball outside of the campus with Japanese people, went to one lab member's live performance, and had parties with all the lab members. All those memories are very precious to me.

JUACEP program provided many meaningful activities. The program staff Kato-san took us to Toyota factory and allowed us to see the culture and trending technology of one of the most famous automobile companies. Kato-san also took us to the Tokugawa art museum where a large collection of treasures and artwork inherited by the family of the daimyō class in the late Edo period were presented. In addition, the program provided us a chance to hand assemble combustion engine, which gave me a better understanding of the mechanism.

The program schedule gave a few long weekends that allow me to visit places outside of Nagoya. One weekend I went to Fuji Mountain with friends. And one weekend I had a chance to visit Kyoto/Osaka area, and enjoyed the sceneries there. During the past ten weeks, I was truly charmed by the culture and humanities in Japan. If you are planning to apply this program, Please do not hesitate. I promise you will have an unforgettable experience here.

(b) Questionnaires

For Q1-4, we asked the same questions BEFORE and AFTER the program.

Q.1: Are you interested in studying at a Japanese university for PhD?

Before

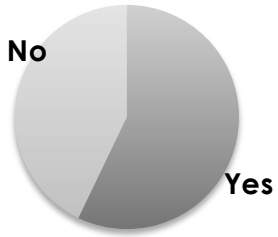

After

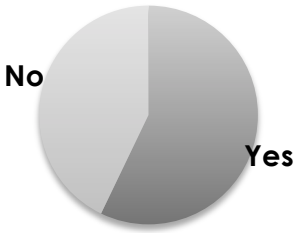

Q.2: Are you interested in working at a Japanese company in USA?

Before

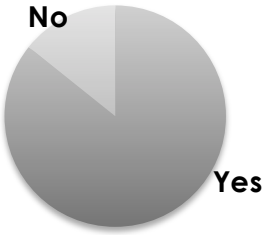

After

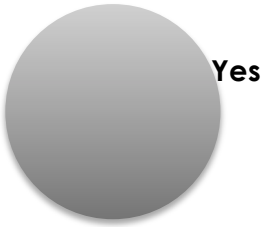

Q.3: Are you interested in working at a Japanese company in Japan?

Before

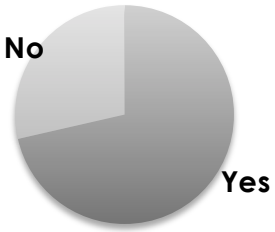

After

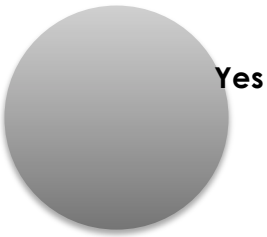

Q.4: Are you interested in working at a non-Japanese company in Japan?

Before

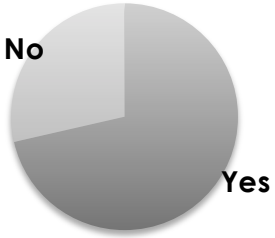

After

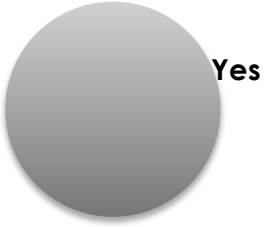

Q.5: Which activity did you like? ('Research internship', 'Field trip', 'Engine assembly', 'Japanese course', others)

- I really enjoyed the internship and field trip together. They are fun and educational. I hope I could have more of them.

- I hope more activities with the JUACEP members. It will be a lot fun.

> Everybody liked and enjoyed almost all activities. Especially 'field trip' was requested with more time and more company/plant tour.

Q.6: In what did you find difficulty? What could be improved? (Excerpts)

[Pre-arrival preparation]

- Since this was my first time to come to Japan, I was not so sure about what should be prepared before the trip: how much money needed initially; how to get a SIM card, and so on. If there is an orientation to get some advice from people who already finished in the past years and get a chance to meet other participants before coming to Japan, that would be much better.

> *-- For your preparation, we introduce you past participants' contact before a couple of weeks of starting the program. You can ask them freely and they are happy to answer. (JUACEP)*

[Language barrier]

- The housing communication can be improved. I found it was difficult to interact with the housing staff due to language barrier.

- Some Japanese don't speak English well.

- Most difficulties I faced were with communication but I learned not to be shy and try to communicate and wish for the best.

- The Japanese class is something that I struggled with, but it was also incredibly rewarding and helpful for adapting to Japanese culture.

[Research circumstances]

- The advising professor is so nice and friendly. I feel free to talk about anything with him. Also assigned adviser always gave me good and effective advice and guidance on my research, which helped me move on smoothly.

[Program period]

- Period to stay is too short. I hope I could stay here and do research for a longer time to explore more new things.

[Others]

- Application system could be built then most of the paper work could be completely done online, which could save efforts of both your office and applicants.

- Payment method for dormitory can be improved. Cash deal only is inconvenient.

Q.7: Write comments freely.

- I appreciate this opportunity to study and live in Japan. Thank you.

- This program is very good and meaningful to me. Not only did I get a chance to see Japan and experience Japanese culture here, I also learned a lot more than just research and traveling part. I felt hospitality from people around me.

- The assigned professor kindly gave me some good advice on sightseeing in Japan at the beginning of the program.

- I felt so warm and grateful when I got back my lost scholarship due to my carelessness on the first day of the program. My TA always stayed with me to give me a hand when I met some difficulties. He also shared me some interesting stories about Japanese culture.

- If possible I'd like to have the ability to go to more field trips to different companies and learn about the research and development that they do in Japan and/or abroad. This would be extremely interesting and provide insights into career opportunities in Japan.

- There could be more diverse student body where not just three institutions are included.

- Even I find difficulty, the people are very friendly here.

- I really hope more people are able to know this program. Thanks for providing me this opportunity.

<5> Appendices

(a) Photo Collection

Orientation & first meeting with lab members, June 19

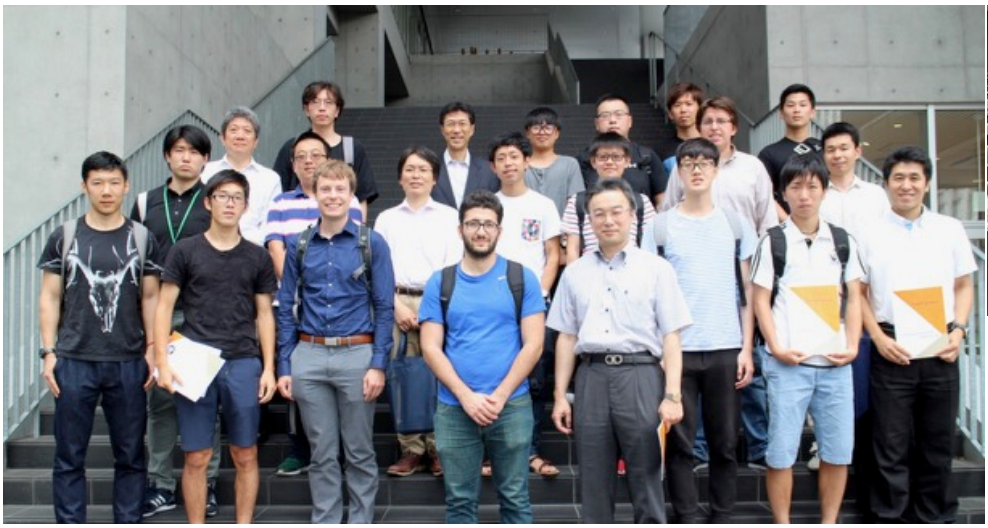

University dormitory ‘Residence Yamate’

Hands-on Exercise 'Internal combustion engine', July 9

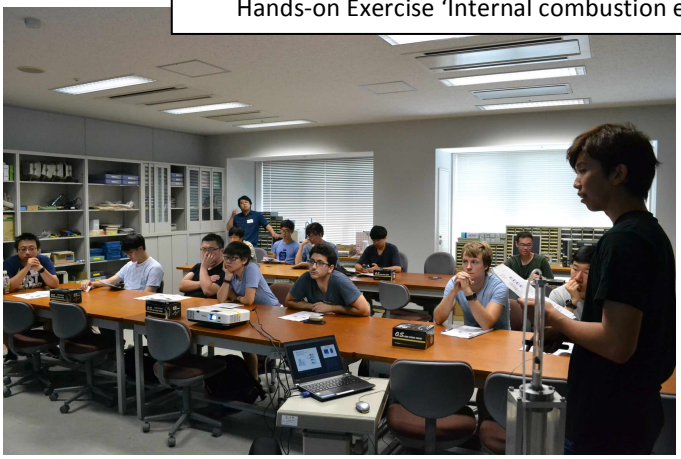

Lectures by TAs

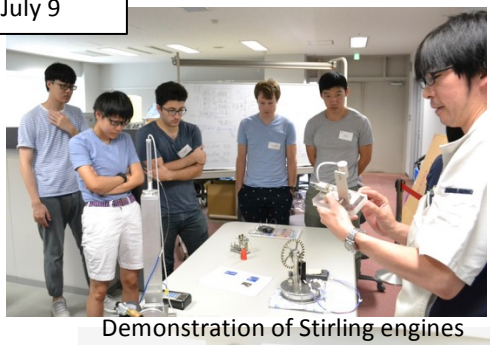

Demonstration of Stirling engines

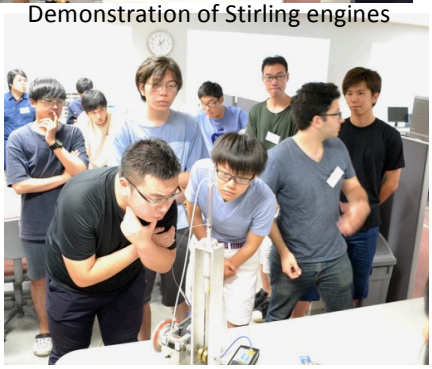

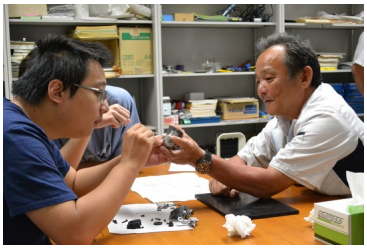

Disassembly and assembly of the engine model

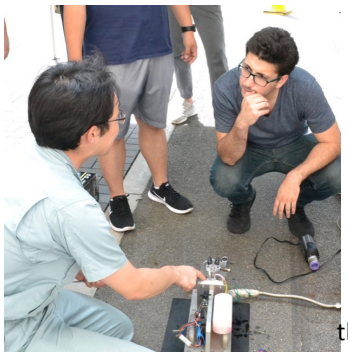

Performance test of the assembled engines

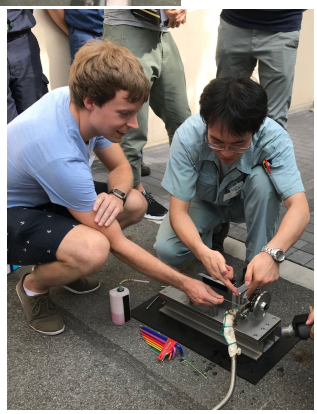

Demonstration of the Jet engine

The 45th JUACEP Seminar by
Prof. Kurabayashi, Univ. Michigan, July 12

Meet-up of US, Canada, JP JUACEP participants, July 12

Field trip: Toyota plant tour, Asahi Brewery tour, Tokugawa Museum, July 27

Toyota Kaikan Museum

Asahi Brewery

Tokugawa Museum

Tasting Asahi beverages

The 47th JUACEP Seminar talked by Prof. YH. Xie, UCLA, August 20

Discussion on the program with Prof. JM. Yang, UCLA, August 21

Address from Dean of Engineering, Prof. Mizutani

The 22nd JUACEP Workshop, August 27, NIC Conference Room

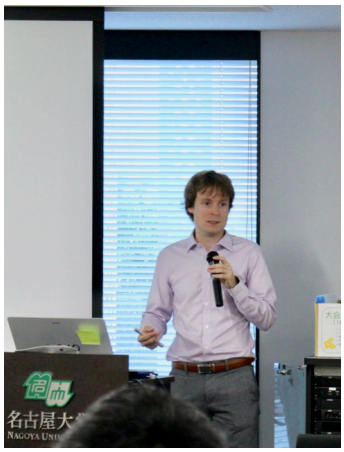

Achievement presentations...Questions and answers

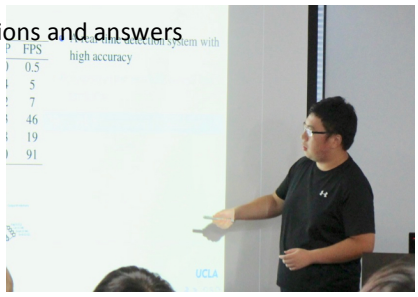

Completion ceremony

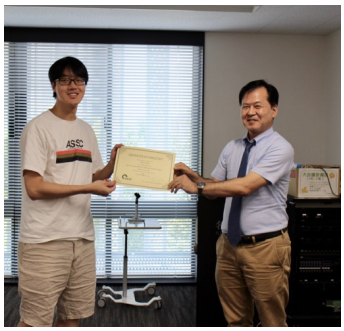

(b) Building Locations

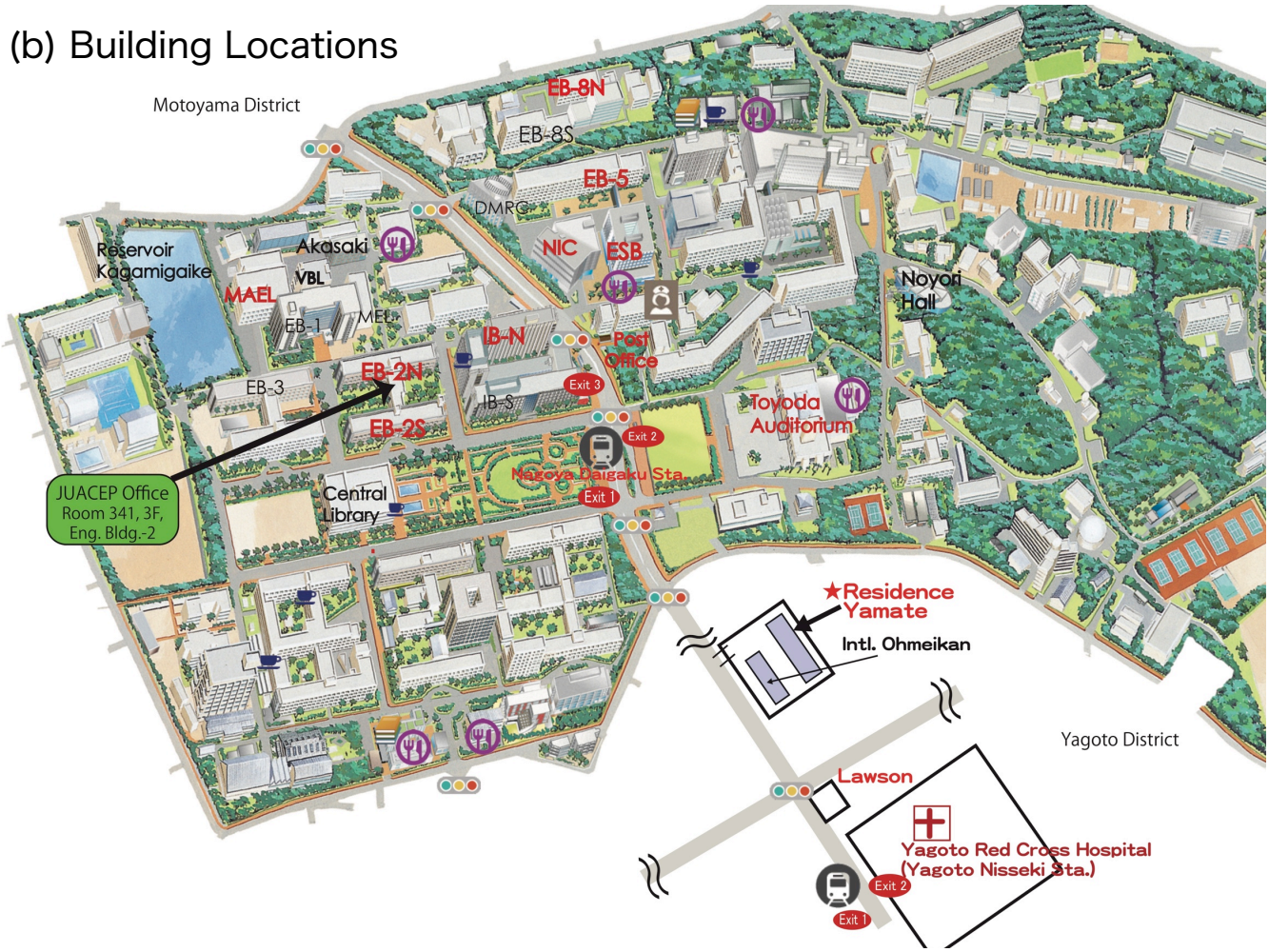

Bldg. icon on the map	Building name (in Japanese)	Important places for JUACEP	Lab locations for JUACEP students
EB-2N	Engineering Building 2 (Kougakubu ni-gou-kan, Kita)	JUACEP Office, 341, 3F Meet-up, July 13 at 424, 4F	Yamada Lab, 3F for Xuan and Guanqun
EB-2S	Engineering Building 2 (Kougakubu ni-gou-kan, Minami)	45th JUACEP Seminar, July 12 at 221, 2F 47th JUACEP Seminar, Aug.22 at 221, 2F	Ju Lab, 1F for Pieter
EB-5	Engineering Building 5 (Kougakubu go-gou-kan)		Usami Lab, 4F for Eddie
EB-8N	Engineering Building 8 (Kougakubu hachi-gou-ka, kita)		Miwa Lab for Ziming
MAEL	Mechanical & Aerospace Engineering Lab. (Kikai kouku jikkentou)		Hasegawa Lab, 2F for Fadi
ESB	Engineering & Science Building (E-S kan)	Orientation, June 19 at ES Hall, 1F Stipend, 13:00, Jul.4 & Aug.3 at SL032, 3F	
NIC	National Innovation Complex (Nic)	22nd Workshop, Aug. 27 at Meeting Room, 3F	
IB-N	Integrated Building North (IB Kita-kan)	Japanese class, 13:45-16:15 at IB101, 10F Hands-on Execises, 13:00, Jul.6&9, 10F	Niitsu Lab, 4F for Star
Toyoda Auditorium	(Toyoda koudou)	Meeting point for Excursion, 9:00, Jul.27	
Post Office		Money change, Money withdrawal, Postal affairs	
	Cafeteria/Convenience Shop		
	Café		
	Book Store		
	Subway Station	Nagoya Univ.: NagoyaDaigaku Station Dormitory Yamate: Yagoto Nisseki Station	
	Health Administration Office	Open hours: 9:00-12:00, 13:00-17:00, Mon.-Fri. (052)789-3970	

Mandatory Deliverables

★ All of following templates can be downloadable at
http://www.juacep.engg.nagoya-u.ac.jp/downloads/index.html

1. JUACEP Independent research report

See *Appendix-1.*
Deadline: **August 28, 2018**
Send to… juacep-office@engg.nagoya-u.ac.jp

2. JUACEP Research presentation slides

We will collect your PowerPoint/PDF slides at the workshop site, **August 27, 2018**.

Evaluation: your final score is calculated by the points of the research report and the presentation at the workshop evaluated by your Nagoya Supervisor;

Research report (1~50pts.) + Presentation (1~50pts.)
100~90=S, 89~80=A, 79~70=B, 69~60=C, 59~0= fail

You will be officially awarded credits of Nagoya University and the transcript is airmailed to your home university in September 2018.

Important:

(a) JUACEP will publish the participants' research reports and the presentation slides in the website and booklet. Please let us know if your supervisor permits its publication by August 28.
(b) UM students MUST transfer the credits to ME590/Engr591 and submit the transcript to JUACEP Office as soon as possible.

3. Findings through JUACEP

Deadline: **August 28, 2018**
Send to… juacep-office@engg.nagoya-u.ac.jp
Please write freely about your experience in Japan inserting pictures.

4. JASSO Scholarship obligatory questionnaires, H-2

There are "Pre-arrival" part which you already submitted and "After the program" part which you have to submit until **August 28, 2018.**
Send to… juacep-office@engg.nagoya-u.ac.jp

Published in December 2018

Japan-US-Canada Advanced Collaborative Education Program (JUACEP)
Graduate School of Engineering
Nagoya University
Furo-cho, Chikusa-ku, Nagoya 464-8603, Japan
JUACEP@engg.nagoya-u.ac.jp
http://www.juacep.engg.nagoya-u.ac.jp